C.P. No. 404
(19,942)
A.R.C. Technical Report

C.P. No. 404
(19,942)
A.R.C. Technical Report

MINISTRY OF SUPPLY

AERONAUTICAL RESEARCH COUNCIL

CURRENT PAPERS

Critical Flight Conditions and Loads Resulting from Inertia Cross-Coupling and Aerodynamic Stability Deficiencies

by

W. J. G. Pinsker

LONDON: HER MAJESTY'S STATIONERY OFFICE

1958

SIX SHILLINGS NET

C.P. 404

U.D.C. No. 533.6.013.413 : 533.6.013.415 : 533.69.048.1

Technical Note No. Aero.2502
March, 1957

ROYAL AIRCRAFT ESTABLISHMENT

Critical flight conditions and loads resulting from inertia cross-coupling and aerodynamic stability deficiencies

by

W. J. G. Pinsker

Paper presented to the Structures and Materials Panel of AGARD at Copenhagen, April 1957

SUMMARY

The effects of the gyroscopic forces on aircraft with large inertias during rolling manoeuvres are discussed and criteria given for the three resulting divergent flight conditions: yaw divergence, pitch divergence and autorotational rolling. The critical loading cases in practical rolling manoeuvres are discussed and methods for the determination of peak loads outlined.

Aircraft responses in inadvertent pitch up are analysed and data are given for the estimation of peak loads both for uncontrolled conditions and for pitch up with pilot's counteraction.

The principal causes for loss of directional stability are indicated and possible dangerous flight conditions are outlined.

LIST OF CONTENTS

LIST OF APPENDICES

LIST OF ILLUSTRATIONS

LIST OF ILLUSTRATIONS (Contd)

1 Introduction

The advent of the transonic and supersonic aircraft has brought with it drastic changes both in the shape and in the mass-distribution of modern designs. Moreover the aerodynamic stabilities vary markedly for supersonic, transonic and subsonic flight.

To avoid excessive stability it is often necessary to accept marginal conditions with the supersonic aircraft at some part of its speed range. The aerodynamicist is of course endeavouring to remedy these faults and the associated critical flight conditions. In many cases, however, he may not be too successful and the structural engineer will have to design adequate strength into the airframe to withstand the loads resulting from these flight conditions.

The most conspicuous design features responsible for the inadvertent response characteristics of the modern aircraft are in particular:

(i) In order to accommodate the increasing amount of loads and equipment of the high speed aircraft behind a minimum of frontal area, fuselages tend to be more elongated and more densely loaded all along their axis. As a result inertias in pitch and in yaw have been increasing steadily without being balanced by increases in the corresponding aerodynamic stabilities. As a consequence, inertia effects tend to be more prominent in aircraft dynamics creating novel and generally undesirable flight conditions.

(ii) As the centre of pressure at the wing moves rearward from subsonic to supersonic flight, the stability margin becomes excessively large. In order to reduce it to the lowest possible level, rather marginal values will usually be tolerated in subsonic flight.

(iii) The progressive reduction in the lift slope of the stabilizing surfaces with increasing supersonic Mach number will lead to gradual loss of directional stability[4].

(iv) As fuselage fineness ratio increases in relation to the size of the tail surfaces, vortices shed from the body will more seriously interfere with the efficiency of these surfaces. This and other aerodynamic interferences will affect in particular the fin so that directional stability diminishes with increasing incidence. This is most undesirable at high speeds where the basic value of n_v is already reduced due to (iii).

(v) The thin airfoil sections and swept planforms of modern wings are prone to localized flow separations, which lead to loss of longitudinal stability at incidences well within the aerodynamically useful range of lift coefficients[3].

(vi) The increased incidence range of the small aspect ratio wing makes it increasingly difficult to locate the horizontal tailplane in a region sufficiently removed from the downwash field behind the wing. Again this may lead to pitch up characteristics similar to those described under (v).

This increased incidence range has also an accumulative effect on inertia cross-coupling phenomena, which will increase in severity with the degree of misalignment of the principal inertia axis with the flight path.

As distinct from the customary treatment of aircraft responses by "classical stability" theory, the phenomena discussed in this paper are associated with non-linearities in the differential equations. As a consequence the prediction of aircraft responses and loads resolves into tedious computations by numerical processes making electronic computations essential. In this situation it is most essential to understand the nature of the problem well so as to be able to select with assurance the really critical cases for more thorough analysis.

In this paper an attempt will be made to give criteria for the assessment of these critical flight conditions and to suggest methods for the estimation of aircraft loads.

2 The physical basis of inertia cross-coupling

The phenomena associated with inertia cross-coupling have only recently been understood after some flight incidents could no longer be explained by conventional theories. The occurence of inertia cross-coupling was first predicted by Phillips in Ref.1, where he shows that aircraft inertia effects couple the lateral and longitudinal modes in the presence of rolling and that this will lead finally at certain critical rolling velocities to yaw and pitch divergencies. Before discussing these theories in greater detail, it is possible to explain these effects by simple qualitative analysis.

The inertia cross-coupling terms appear in the Euler equations of the aircraft motion[2] as products of variables. Using principal inertia axes as illustrated in Fig.1 for simplicity of analysis these are:

$$L = A\dot{p} - (B-C)\,qr \tag{1}$$

$$M = B\dot{q} + (A-C)\,rp \tag{2}$$

$$N = C\dot{r} - (A-B)\,pq \tag{3}$$

$$X = \left(\frac{\dot{u}}{V} - \alpha\beta\right) mV \tag{4}$$

$$Y = (\dot{\beta} + r - p\alpha)\, mV \tag{5}$$

$$Z = (\dot{\alpha} - q + p\beta)\, mV \tag{6}$$

In accordance with the concept of small perturbations in the past products of variables have generally been omitted from stability analysis. This simplification was highly desirable as then the longitudinal and lateral equations could be separated and these motions considered independently.

However, rate of roll p can be large when compared with unity so that at least the products with p may have to be taken into account, if the associated inertia terms are sufficiently large.

2.1 The physical origin of the aircraft gyroscopic terms

This leaves four cross-coupling terms to be considered:

$$\Delta M = (A-C)\,rp \tag{7}$$

$$\Delta N = (B-A)\,pq \tag{8}$$

$$\Delta Y = -p\alpha\, mV \tag{9}$$

$$\Delta Z = p\beta\, mV \tag{10}$$

The first two of these terms are gyroscopic couples, which can be easily understood by reference to Figs.2 and 3.

In Fig.2 the inertia distribution of an aircraft is represented by two pairs of concentrated masses, m_C, to represent inertia in yaw (C) and m_A

to represent inertia in roll (A). For convenience of pictorial representation the rolling inertia couple m_A is shown in the plane of symmetry of the aircraft, i.e. normal to the wing plane which normally contains the rolling inertia, but this does not affect the argument. Now, if rate of roll p and rate of yaw r are present simultaneously, they add up to a resultant angular velocity Ω. Thus the aircraft spins with Ω about an axis inclined at an angle $\alpha = \tan^{-1}(r/p)$ with respect to the principal inertia axis. The yawing inertia couple m_C will now be subject to centrifugal forces exerting a nose up pitching moment M_C if both p and r are positive - as illustrated, or if they are both negative. If p and r have opposite signs the resulting pitch will be nose down ($M_C < 0$). As seen from Fig.2 the rolling inertia couple M_A will always oppose the yawing inertia couple M_A, as expressed in equation (7).

A similar argument can be applied to explain the term $N = (B-A)\,pq$. In Fig.3 the aircraft inertias in pitch B and roll A are again represented by pairs of masses m_B and m_A. Simultaneous rotation in roll p and in pitch q results in an angular motion subjecting these masses to centrifugal forces. The pitching couple m_B will produce negative yawing N_B and the rolling couple m_A positive yawing N_A, if p and q have both the same sign and vice versa.

The two remaining product terms $p\alpha$ and $p\beta$ can simply be interpreted as kinematic relations: $\dot{\beta} = p\alpha$ and $\dot{\alpha} = -p\beta$ as illustrated in Figs.4 and 5. In Fig.4 an aircraft rolls about its fuselage axis starting from an initial incidence α_o. This is seen to lead to a build up in sideslip. Similarly in Fig.5 rolling with an initial sideslip β_o is seen to lead to a build up in negative incidence.

2.2 Pitch and yaw divergence in rolling

With the concepts derived in the preceding section the generation of inertia induced aircraft divergencies can easily be visualized.

As an introduction the more conventional case of an aircraft with strong static stability both in yaw and in pitch (or negligible inertias) is illustrated in Fig.6. The aerodynamic restraints will retain incidence and sideslip constant throughout the rolling manoeuvre. The motion is stable.

To go to the other extreme, consider now an aircraft with very pronounced inertias and negligible aerodynamic stability. The aircraft rolls about its principal inertia axis which will retain its position in space and thereby enforce a periodic interchange of α and β. The motion again is stable. The same situation arises with an aircraft with less extreme combinations of inertias and aerodynamic restraints, if one rolls it fast enough, so that the aerodynamic forces have little time to act on the aircraft, whilst the gyroscopic forces are amplified as they increase with the square of the rolling velocity.

The phenomena referred to as inertia cross-coupling arise generally from a situation half way between the two extremes discussed so far. They are the result of an unfortunate interplay between inertial and aerodynamic effects.

This is illustrated in Fig.8 for an aircraft with inadequate longitudinal stability. The motion again is steady rolling starting with an initial incidence α_o at stage I. After rolling through 90° (II) the aircraft would have developed sideslip as indicated by the dashed outline. As this aircraft is assumed to possess powerful directional stability n_v, this will force the aircraft directionally back unto the flight path by

imposing a rate of yaw. This rate of yaw r will combine with rate of roll p to an angular velocity Ω, under the influence of which the yawing inertia couple m_C will produce a nose up pitching moment, increasing the aircraft incidence. If the aerodynamic restoring moment in pitch is too weak to hold the aircraft against this inertia couple, the motion will become divergent.

An analogue reaction will take place in the case illustrated in Fig.9, where m_W is assumed very powerful and n_v inadequate. Starting the motion from an initial displacement in sideslip, the pitching inertia couple m_B is seen to produce a yawing moment in a sense to increase the initial sideslip. If n_v is below a certain level, the motion will become divergent in yaw.

The rolling inertia couple (not represented in Fig.9) will counteract the effect of the pitching inertia couple in this condition. If as illustrated in Fig.10 A is larger than B, the motion will be stabilized even in the absence of directional stability.

2.3 Autorotational rolling

To add further to the previously discussed list of discomforts inertia cross-coupling is also capable of destabilizing the rolling motion itself. This phenomenon has not yet made any dramatic appearance in flight, but there are indications that the autorotational rolling states predicted by theory may afflict the next generation of aircraft.

This motion may again be visualized by the technique used for the pitch and yaw divergences. In Fig.11 an aircraft is depicted rolling steadily from an initial negative incidence α_o at stage I. Rolling through 90° (stage II) negative sideslip will have developed. Directional stability n_v tends to restore alignment with the flight path by imposing negative rate of yaw on the aircraft. As n_v is not infinitely strong some sideslip will remain. In stage III rate of yaw and roll are seen to combine to give an aircraft rotation Ω which releases, via the yawing inertia couple, a nose down pitching moment. In stage IV this is seen to have increased the negative incidence, the resulting negative lift will enforce a negative pull-out with a rate of pitch q. (As the motion will stabilize itself into a steady state, this will produce a "barrel roll".) In stage V rate of pitch and roll are combining to an angular rotation displaced directionally from the fuselage axis and the pitching inertia couple will release a yawing moment N_B. Finally this yawing moment (stage VI) will lead to an increased sideslip in a sense that the resulting rolling moment due to sideslip ℓ_v will assist the rolling motion, provided ℓ_v at the large negative incidence reached at this stage is still negative.

This sequence will lead to an autorotationally stable state for certain combinations of the parameters involved. This is analysed numerically in Section 3.2 of this paper.

3 Stability criteria for gyroscopically induced aircraft modes

The equations of motions to be considered for numerical analysis, retaining only those terms which have been found to be significant, are as follows:

$$L_\beta \beta + L_r r + L_p p - A\dot{p} = - L_\xi \xi$$

$$M_\alpha \alpha + M_q q + M_{\dot\alpha} \dot\alpha + (C-A)\, pr - B\dot{q} = - M_\eta \eta \qquad (12)$$

$$N_\beta \beta + N_r r + N_p p - (B-A)\, pq - C\dot{r} = - N_\zeta \zeta - N_\xi \xi \qquad (13)$$

$$\frac{Y_\beta}{mV} \beta - r - \dot\beta + p\,(\alpha_o + \Delta\alpha) = 0 \qquad (14)$$

$$\frac{Z_\alpha}{mV} \Delta\alpha + q - p\beta - \dot\alpha = 0 \qquad (15)$$

Being non-linear these equations cannot be readily analysed. In the above form they are, however, the equations to be solved in response calculations. Making certain simplifying assumptions, useful generalized stability criteria can, however, be obtained, which will be sufficient to allow a first assessment of an aircraft's proneness to inertia cross-coupling effects.

3.1 Pitch and yaw divergence

Assuming steady rates of roll $p = p_o$, the rolling moment equation (11) becomes redundant and the remaining four equations linear with p_o as a parameter. A simple solution for the case of zero aircraft damping is given in Appendix I. This process as suggested by Phillips[1] gives the most fundamental criterion to say that there will be a divergence predominantly in pitch if

$$\omega_\theta < p_o < \omega_\psi \sqrt{\frac{C}{B-A}} \tag{16}$$

or a divergence predominantly in yaw if

$$\omega_\theta > p_o > \omega_\psi \sqrt{\frac{C}{B-A}} \tag{17}$$

whichever case applies. In these equations:

$\omega_\theta = \frac{2\pi}{T_\theta}$ = angular frequency of the uncoupled pitching oscillation

$\omega_\psi = \frac{2\pi}{T_\psi}$ = angular frequency of the uncoupled directional oscillation

p_o = steady rate of roll in rad/sec.

In words that is to say that the aircraft will become unstable if rates of roll (in rad/sec) exceeds numerically the lower of the two frequencies of the basic modes of the aircraft, whereby in the case of the lateral frequency the critical rate of roll is further increased by the alleviating influence of inertia in roll. The corresponding stability diagram is given in Fig.12. The beneficial effect of A is shown there by the fact that the vertical (yaw stability) boundary is moved towards the origin as A increases in relation to B.

The broad trends in the relation of A : B in aircraft design over a period of 20 years are shown in Fig.13. It is clearly seen that in the past the occurence of the yaw divergence was delayed by more favourable inertia in roll contributions, even if the other aircraft parameters would have encouraged this phenomenon.

The interpretation of the stability diagram may be assisted by the sketch in Fig.14, which illustrates the case of three distinct aircraft configurations.

Aircraft "A", the most common case where $\omega_\theta >> \omega_\psi$ i.e. $n_v << m_w$ Increasing rate of roll, i.e. moving radially towards the origin of the diagram, the vertical boundary is first struck at the critical roll rate and for a range of p_o above this value the aircraft will show a divergence in yaw until finally at very high rates of roll the motion would again be stable. This condition is most likely to occur in supersonic flight where n_v tends to decrease and m_w is very large.

Aircraft "B" exhibits the opposite tendencies. Here $\omega_\theta << \omega_\psi$ and the instability will be predominantly in pitch leading to large normal accelerations.

Aircraft "C" illustrates an interesting condition. By "tuning" directional and longitudinal stability so that $\omega_\theta = \omega_\psi \sqrt{\frac{C}{B-A}}$, i.e. $m_w \ell = n_v \frac{b}{2} \frac{C}{B-A}$ stability is assured for the full range of rolling velocities. The designer is of course aware of this escape route and will tend to utilize it, other considerations permitting. Unfortunately this tuned condition can normally only be maintained over some part of the speed range, as inevitable changes in the aerodynamic derivates with Mach number etc. will change the ratio of $m_w : n_v$. It should also be pointed out here, that, although no actual divergence occurs, the response of an aircraft rolling anywhere near the unstable conditions will most likely exhibit amplitudes in incidence or sideslip which are large enough to constitute a stressing hazard.

The effect of the other parameters might be best discussed by rewriting the two critical rolling condition in the form

$$p^2 < \frac{n_v}{i_B \left(1 - \frac{A}{B}\right)} \frac{V_i^2}{W/S} \frac{b/2}{\ell^2} 0.0765 \qquad (18)$$

and

$$p^2 < -\frac{m_w}{i_B} \frac{V_i^2}{W/S \ \ell} 0.0765 \ . \qquad (19)$$

Large static stability derivatives n_v and m_w are obviously beneficial and so is speed. When considering speed it must, however be realized that the loads might be larger in a mild instability at high speeds than in a rapid divergence at low speeds.

Finally there are two further parameters influencing the stability boundaries, but none of these to a very dramatic extent.

Aircraft damping in pitch and yaw will separate the two unstable regions as illustrated in Fig.15. As a consequence there is now a greater margin for tuning the aerodynamic stabilities to avoid divergence.

The effect of the momentum of the rotating parts of an engine is shown in Fig.16. This effect is asymmetric, i.e. for rolling in a sense opposite to the engine rotation divergence occurs at a slightly lower rate than in the case where aircraft and engine rotate in the same sense. It has been suggested to represent engine momentum by interpreting the parameters:

$$\left(\frac{\omega_\theta}{p_o}\right)^2 \quad \text{to read} \quad \left(\frac{\omega_\theta}{p_o}\right)^2 + \frac{I_e \ \omega_e}{B \ p_o} \qquad (20)$$

and

$$\left(\frac{\omega_\psi}{p_o}\right)^2 \quad \text{to read} \quad \left(\frac{\omega_\psi}{p_o}\right)^2 + \frac{I_e \ \omega_e}{B \ p_o} \qquad (21)$$

where $I_e \omega_e$ is the angular momentum of the engines. For an assessment of the more severe condition rolling in the sense opposite to the engine rotation should be considered.

3.2 Autorotational rolling

In Appendix II the existence of autorotational rolling states under the influence of inertia cross-coupling is proved. These are basically possible if an aircraft flies with an incidence of its principal inertia axis below a critical value which can be read from the graph in Fig.17. As this phenomenon is thus largely confined to flight under negative incidence, it is most likely to be met in pushover manoeuvres or with aircraft layouts featuring an inherently negatively inclined principal inertia axis. It is interesting to note that tuning m_w and n_v will again give the least unstable condition, although the instability cannot be completely removed, provided the negative incidence is made large enough.

For the condition with negligible aircraft damping the critical rolling velocities are plotted in Fig.18 against the relevant parameters. The dotted lines represent the minimum rates of roll at which the rolling motion becomes divergent and the full lines give the rates of roll at which the motion would become autorotationally stable. The practical significance of this phenomenon to the pilot is not fully understood yet, but it can be shown that in quite realistic designs the critical roll rate may be of the order of 20°/sec.

For the structural designer there are two significant consequences:

(i) Even if available aileron power does not permit exceeding of the critical roll rates, inertia cross-coupling effects will tend to reduce effectively roll damping so that higher roll rates may be achieved with a given aileron power and the aircraft may have to be stressed for these.

(ii) If the critical roll rate is within the ailerons power, the possibility of the aircraft inadvertently attaining the steady autorotational rate must be considered, even if it seems possible that the pilot will regain control, so that the condition could be tolerated as a handling nuisance.

4 Aircraft loads in cross-coupled rolling manoeuvres

The stability criteria discussed before for the conditions of yaw and pitch divergence in steady rolling can serve as a useful and reliable guide to assess the probability of a given aircraft to be seriously impaired by inertia cross-coupling. If the stability criteria show the aircraft to be safely clear of regions of reduced stability, inertia cross-coupling may be dismissed from stressing considerations. In all other cases and of course in case of doubt, the more critical manoeuvres must be fully computed and evaluated for peak loads. Unfortunately at this juncture the problem ceases to be simple and tedious numerical work must be faced. If electronic computors are available, this task becomes manageable. The solution will be found by computing equations (11) - (15) for all desired control manoeuvres. However, in addition to the stability criteria discussed there are still some further more generalized conclusions, which may help to understand better the particular problems of aircraft response in controlled manoeuvres and so to short-cut somewhat the final computations.

Obviously at low speeds, where structural integrity is inherent up to the stall both in incidence and in sideslip there is no stressing case and the problem can be left with the aerodynamicist. On the other hand relatively small disturbances will at high speeds produce quite

intolerable loads. It is therefore most important not to overlook a relatively innocent flight condition if it is associated with high speeds.

As the aircraft response deteriorates rapidly as the critical conditions are approached, in borderline cases it is wise to use the most pessimostic estimates for the aerodynamic derivatives and for the inertia distribution.

In cross-coupled rolling the aircraft is likely to experience large disturbances in incidence and sideslip. Non-linearities and changes of derivatives with these parameters may have to be taken into account, such as non-linear pitching moments and variations of e.g. n_v with incidence.

4.1 Trimming the aircraft in rolling manoeuvres

A quick assessment of the magnitude of the problem is possible by estimating the forces required to hold the aircraft during rolling in its initial trimmed condition. In Appendix III the rudder and elevator movements required to perform a rolling manoeuvre with constant incidence and zero sideslip throughout are determined as:

$$\text{Rudder:} \quad \zeta(t) = \frac{C}{N_\zeta} \alpha_o \dot{p}(t) - \frac{n_\xi}{n_\zeta} \xi(t) - \frac{n_p}{n_\zeta} \frac{b/2}{V} p(t) \qquad (22)$$

$$\text{Elevator:} \quad \eta(t) = - \frac{C - A}{M_\eta} \alpha_o p^2(t) \ . \qquad (23)$$

Thus apart from the conventionally known effects of n_ξ and n_p a yawing moment proportional to acceleration in roll $\dot{p}$ and to the incidence of the principal inertia axis α_o must be held. Elevator must be applied to hold a pitching moment proportional to α_o and to the square of rate of roll. This is illustrated by an example based on a current design in Fig.19. The trim forces indicated for this condition are quite formidable, a good indication of the severity of the case.

Equations (22) - (23) reveal, however, two trends which are a reflection of similar effects to be observed in general response and load estimations in cross-coupled rolling. The disturbances imposed upon the aircraft by the gyroscopic inertia forces are proportional to α_o and so as a consequence are the incremental loads resulting from such manoeuvres. The yawing excitation is further proportional to acceleration in roll, thus the more rapid a rolling manoeuvre is initiated and also terminated, the greater aircraft disturbances and therefore loads are to be expected. This again is generally found in all response computations.

4.2 Peak loads in banking and rolling manoeuvres

Here we will give the conclusions drawn from a large number of response calculations on aircraft subject to inertia cross-coupling. The majority of these computations were based on the assumption that rate of roll is largely governed by the isolated rolling moment equation, which can be considered separately and that the aircraft response in pitch and yaw is then adequately determined by treating rate of roll as an independent variable. For a given time history $p(t)$ i.e. for a given rolling manoeuvre the aircraft response is then found by computing:

$$M_\alpha \Delta\alpha + M_q q + M_{\dot\alpha} \dot\alpha + (C-A)\, p(t)\, r - B\dot q = 0 \qquad (24)$$

$$N_\beta \beta + N_r r - (B-A)\, p(t)\, q - C\dot r = -N_p p(t) \qquad (25)$$

$$\frac{Y_\beta}{mV} \beta - r - \dot\beta + p(t)\, \Delta\alpha = -p(t)\, \alpha_o \qquad (26)$$

$$\frac{Z_\alpha}{mV} \Delta\alpha + q - \dot\alpha - p(t)\, \beta = 0 \qquad (27)$$

if the elevator and rudder are assumed fixed. Mathematically this represents a system of linear differential equations with time-variable coefficients. The terms on the right hand side represent the excitation functions. As the equations are linear, solutions to the two input terms both varying with $p(t)$ can be treated separately and then superimposed linearly. It has generally been found that the contribution of N_p is rather small when compared with that due to the α_o term, so that it is generally true that the response amplitudes in incidence and sideslip and the corresponding loads are proportional to the initial incidence α_o of the principal inertia axis. Thus the loads expected in a pull-out under ng can be simply deduced from the loads computed for a similar rolling manoeuvre at 1g by increasing these by the ratio of the incidences in the two flight conditions, e.g.

$$\frac{\Delta\alpha_{max}(ng)}{\Delta\alpha_{max}(1g)} = \frac{\alpha_o(ng)}{\alpha_o(1g)} . \qquad (28)$$

The response and the loads in incidence $\Delta\alpha(t)$ are independent of the sense of the rolling motion, sideslip changes sign with the sign of p. This neglects of course the effect of the engine momentum, which as shown earlier makes the response slightly asymmetric for port and starboard rolling.

A typical time history of an inertia-cross-coupled rolling manoeuvre is shown in Fig.20. This illustrates another significant general observation, namely that the peak amplitudes in incidence and sideslip occur frequently after the termination of the rolling manoeuvre. Computations must therefore be continued until the aircraft motion is without doubt damped out. As already mentioned, the more abruptly rolling is initiated and terminated (in particular the latter) the greater will be the load peaks.

The duration of the rolling manoeuvre is another important parameter. Though - as expected - the peak loads increase at first progressively with the duration of the aileron application, this is not necessarily true over the full range. This may be illustrated by the results of response calculations based on the family of rolling manoeuvres illustrated in Fig.21 where the duration t_1 and thus the total bank angle $\Delta\phi$ has been varied systematically. These computations have been carried out for a wide range of aircraft parameters. The peak amplitudes in incidence $\Delta\alpha_{max}$ and sideslip β_{max} have been evaluated and plotted against $\Delta\phi$. These plots have been found to follow three distinct patterns (Fig.22), and that these types are associated with the principal regions in the stability diagrams Figs.14-16, if the parameters ω_θ/p_o and ω_ψ/p_o are based on the final rate of roll p_o in Fig.21, which is rather a nominal value, being only approached for manoeuvres with longer duration.

In flight conditions associated with one of the stable regions the characteristic depicted in Fig.22a was found. In this case the worst response occurs for rolling through a quite modest bank angle (I). If case II, i.e. rolling through about twice this angle would have been considered, a much too optimistic result were obtained which did not cover all rolling manoeuvres up to the computed case. The characteristics found in conditions at the stability boundary (22b) and in the divergent regions (22c) are progressive as would be expected.

The variation of peak loads with rate of roll for an otherwise identical manoeuvre must obviously be related to the traverse through the unstable region of the corresponding loci in the stability diagram, Fig.14. Although for continuous rolling the worst condition would be expected right inside the unstable region, for rolling manoeuvres with limited duration the worst load peaks are usually obtained for rates of roll well beyond the unstable range, as illustrated by two examples in Fig.23.

It is practically impossible to give any general rules on the effects of height, speed and Mach number. Height and low speeds will give the greatest peak amplitudes (provided the aerodynamic derivatives are constant, which of course they are not). This does not, however, necessarily mean maximum loads also, as these increase in proportion to V_I^2, again assuming constant aerodynamic aircraft characteristics. Frequently the most severe stressing case is found at sea level near the top speed, contradicting completely the simple criteria one is tempted to apply. Full exploration of the performance envelope of the aircraft is generally necessary to determine the critical condition.

Increasing the aerodynamic stabilities m_w and n_v is generally beneficial as is apparent from simple stability considerations, but again if only one stability is increased, the relief in the corresponding freedom is frequently bought at the expense of greater loads in the other freedom. Aircraft damping has a mildly alleviating effect, in particular pitch damping. n_r and n_p add, as explained earlier to the other effects in cross-coupling and ought therefore to be kept small.

4.3 Pilot's contribution

Theoretically a pilot would be able to control the aircraft in rolling by applying suitable co-ordinated rudder and elevator movements. A glance at Fig.19 will show, what he would be expected to do and it seems obvious that he has little chance of achieving these movements which are not related to readily perceptible flight sensations and parameters. In general his interference may easily be ill timed and then contributory to inertia cross-coupling rather than corrective. At the present state of the art, pilots should be discouraged from interference and load assessment based on manoeuvres with rudder and elevator fixed.

4.4 Autostabilization

So far no effective autostabilizer has been designed to alleviate significantly the effects of inertia cross-coupling. The principal obstacle is again - as with the problem of pilot's control - the very substantial control authority such a device would have to be given to be effective. Even conventional pitch and yaw dampers are of little value as they have rather limited authority and their contribution would terminate very early in a manoeuvre.

5 Aircraft response and loads in pitch up

The term pitch up is usually meant to describe a nose up pitching motion resulting from loss of longitudinal stability over a part of the incidence range of an aircraft usually below the stall. The aerodynamicist is naturally more concerned with a cure of this phenomenon than with the prediction of loads

resulting from it. As our understanding of the aerodynamic basis of pitch up grows, this unpleasant feature may be controlled in the design stage. For the time being, however, it appears that a number of aircraft will be afflicted with some degree of pitch up and it may be worth considering the aircraft loads arising from pitch up manoeuvres.

Fig.24 shows a typical example of a pitch up characteristic as a localized reversal of the slope of pitching moment C_m against incidence α.

In order to obtain some general ideas on the aircraft response and loads resulting from such a characteristic for ease of analysis this pitching moment curve was represented by the two simplified cases illustrated in Fig.25.

In each of the two cases a stable slope ($M_\alpha < 0$) is assumed up to the critical incidence α_K, beyond which an unstable slope with ($M_\alpha > 0$) is assumed. In the second case considered at an incidence α_R stability would be restored and for $\alpha > \alpha_R$ the pitching moment curve is again stable.

Based on a simple one degree of freedom approximation the stability roots are plotted against static stability M_α and effective damping in pitch $D = {}^{M}q/B + {}^{M}\dot{\alpha}/B + Z_\alpha$ in Fig.26. For unstable M_α the motion is described by two real roots, λ_1 representing the divergent mode and λ_2 the co-ordinated subsidence. This graph will assist in the interpretation of the pitch response data given in the following paragraphs.

5.1 Pilot controlled pitch up

In Appendix IV aircraft response in pitch has been computed for the case where the aircraft is unstable for all $\alpha > \alpha_K$. In the manoeuvre computed, the aircraft is assumed to be initially trimmed in steady flight at exactly the critical incidence α_K. The pilot is assumed not to be aware of the inherent danger and puts on elevator η_o so as to increase incidence. After t_p seconds he has realized the resulting motion is divergent and applied corrective elevator η_R as shown in Fig.27. If this attempt is adequate, i.e. early and powerful enough, an aircraft motion as illustrated in Fig.27a will result with a finite maximum overswing amplitude $\Delta\alpha_{max}$. If he is too late or has not applied enough forward stick movement η_R the pitch up will not be arrested and the aircraft will pitch as shown in Fig.27b into the stall. For ease of analysis the two elevator angles involved are represented by equivalent "trimmed incidences",

$$\alpha_o = \eta_o \frac{m_\eta}{m_w} < 0 \qquad (29)$$

$$\alpha_S = \eta_R \frac{m_\eta}{m_w} > 0 \qquad (30)$$

where $m_w = {}^{\partial C_m}/_{\partial\alpha}$ in the unstable range. These angles can be readily obtained from a pitching moment graph as indicated in the sketch in Fig.29. In Fig.29 the peak values of the incremental incidences $\Delta\alpha_{max}$ are plotted against pilots' time delay t_p times the divergence root λ_1 with the ratio between η_R/η_o as a parameter. A further parameter considered is the ratio of the two roots describing the pitching motion in the unstable condition: λ_2/λ_1. This ratio increases as can be readily seen from

Fig.26 with increasing aircraft damping $M_{\dot{\theta}}$. The data given in Fig.29 can be interpreted in two ways. First they determine the maximum time delay for recovery action permissible to prevent uncontrollable divergence. Secondly they give values of peak amplitudes in incidence for a given recovery action. For this purpose we must make some plausible assumption for t_P, which can be considered to be composed of three contributions:

$$t_P = t_R + t_D + t_C \tag{31}$$

(i) t_R is the time passing before the pilot realises that the motion initiated by him is divergent. This will depend on the violence of the pitch up and as a tentative value $t_R \geq -\lambda_1^{-1}$ may be used.

(ii) t_D, the pilots' inherent reaction time lag is approximately 0.3 secs.

(iii) t_C is the time required to move the stick forward to η_R. This will depend on the stick feel characteristics, as a minimum 0.2 secs may be a reasonable value.

Thus

$$t_P \geq \frac{1}{-\lambda_1} + 0.5 \text{ secs} \tag{32}$$

If we write equation (32) in terms of the parameter used in the response calculations, Fig.29, i.e.

$$\lambda_1 t_P = 1 + 0.5 (-\lambda_1)$$

it can readily be seen that recovery is unlikely for values of $\lambda_1 < -2$ and even then a very considerable amount of countercontrol η_R has to be applied. Thus only a rather mild degree of pitch up of this form would at all be tolerable.

However in many cases the incidence range over which instability exists, is restricted and the aircraft would stabilize itself at an incidence beyond the unstable region.

5.2 Load peaks in a self-stabilizing pitch up

For pitch up restricted to a relatively limited incidence range as shown in Fig.25b, the motion illustrated in Fig.28 was computed. Initially the aircraft is again assumed in steady trimmed flight just at the critical incidence α_K and is then disturbed by the pilot applying elevator η_o, which in this case is held on steadily until the aircraft stabilizes itself in the re-established stable range beyond α_R. The overshoot in incidence resulting from this manoeuvre has been computed in Appendix V and is plotted in Fig.30 against ζ_D the damping ratio of the pitching oscillation associated with the stable range.

The damping ratios of the pitching oscillation of modern high speed aircraft at operational altitudes are generally below 0.25. With a typical value for the parameter $\left\{\frac{\alpha_u}{\alpha_S}\frac{\lambda_1}{\omega_\theta}\right\}$ of approximately 1.0 the overshoot in incidence would then be 100% based on α_S, a quite considerable amount.

Generally the loss of longitudinal stability in the pitch up region leaves the lift curve slope practically unchanged, thus the incremental incidence peak $\Delta\alpha_{max}$ will produce normal g's in proportion to these. For the assessment of tail loads the origin of the instability must, however, be considered in detail. If the deficiency arises from a loss of tailplane efficiency (due to downwash) the tail will be unloaded and the stressing condition is alleviated. If on the other hand the pitch up is generated on the wing itself, tail loads will increase in proportion to the incidence build up and this will then be further enforced by the nose down elevator applied as corrective control.

6 Directional divergence

Deficiencies in directional stability will normally be of a character quite different from those leading to the longitudinal pitch up, which resulted from non-linearities in the restoring moment itself. The more likely case of loss of directional stability is a reduction of the derivative n_v as flight conditions change.

E.g. n_v will be progressively reduced with increasing supersonic Mach number until at some critical speed directional stability disappears altogether. The pilot would be faced as a consequence with an insipient directional divergence and of course long before then with trouble in manoeuvring for instance due to inertia cross-coupling. The aircraft would in this case violate all basic requirements and a fundamental design-remedy is demanded.

A more practical case arises if n_v is reduced with increasing incidence due to induced flows. If the pilot pulls out in such a flight condition he may suddenly find himself without yaw-stability and for the duration of the pull out sideslip will build up in a divergent fashion. If one should decide to accept this case as an acceptable handling hazard, peak loads in sideslip resulting from this manoeuvre can be estimated by methods similar to those outlined with the pitch up.

7 Conclusions

It has been shown that supersonic aircraft are prone to develop unstable flight conditions for which the aerodynamicist might not be able always to find a complete cure. They may then create new stressing cases. The conditions discussed in this paper are:

(i) If aircraft inertias increase in relation to the weathercock stabilities in yaw and in pitch, the aircraft will be liable to divergent pitching and yawing motions during rolling manoeuvres. These phenomena are further encouraged if inertia in roll is small compared with inertia in pitch. The load peaks resulting from inertia cross-coupled manoeuvres increase generally in proportion to the initial incidence of the principal inertia axis and progressively with the duration of the roll and with the rapidity of the aileron application at the beginning and the end of the manoeuvre. The most severe flight conditions are at speeds where compressibility effects or other aerodynamic phenomena reduce either m_w or n_v to marginal values.

(ii) The gyroscopic forces generated by an aircraft with large inertias may also lead to autorotational rolling states predominantly at negative incidences. These rolling states can be easily predicted and may be well above rates of roll for which the aircraft is normally stressed.

(iii) Unstable pitch up characteristics result from aerodynamic deficiencies inherent in a typical supersonic aircraft layout. Data are given to determine whether a given pitch up would be controllable and also to assess the peak loads from pitch up manoeuvres with and without pilot counteraction.

(iv) Loss of directional stability may occur at high supersonic Mach numbers and/or at high incidence. As it generally leads to wholly unacceptable flight conditions, this stability deficiency should basically be cured by design modifications. However, methods of calculating load peaks resulting from localized directional instability are suggested.

REFERENCES

No.	Author	Title, etc.
1	Phillips, William H.	Effect of steady rolling on longitudinal and directional stability. NACA T.N. 1627, June 1948.
2	Duncan, W.J.	The principles of the control and stability of aircraft. Cambridge University Press, 1952.
3	Foster, G.V. and Griner, R.F.	A study of several factors affecting the stability contributed by a horizontal tail at various vertical positions on a swept back wing airplane model. NACA T.N. 3848; NACA RM L9H19, November 1956.
4	Wiggins, J.W., Kuhn, R.E. and Fournier, P.G.	Wind tunnel investigations to determine the horizontal and vertical tail contributions to the static lateral stability characteristics of a complete model swept wing configuration at high subsonic speeds. NACA T.N. 3818; NACA RM L53E19, NACA TIB 3813, November 1956.

Attached:-

Appendices I to V

LIST OF SYMBOLS

A inertia in roll

B inertia in pitch

b wing span

C inertia in yaw

c mean chord

$C_\ell = \dfrac{L}{\rho/2\ V^2\ S\ b}$ rolling moment coefficient

$C_n = \dfrac{N}{\rho/2\ V^2\ S\ b}$ yawing moment coefficient

$C_m = \dfrac{M}{\rho/2\ V^2\ S\ c}$ pitching moment coefficient

I_e inertia of the rotor of an engine

ℓ tail arm

L rolling moment

$L_p = \dfrac{\partial L}{\partial p}$ damping in roll

$L_r = \dfrac{\partial L}{\partial r}$ rolling moment due to rate of yaw

$L_\beta = \dfrac{\partial L}{\partial \beta}$ rolling moment due to sideslip

$L_\xi = \dfrac{\partial L}{\partial \xi}$ aileron power

$\ell_v = \dfrac{\partial C_\ell}{\partial \beta}$ non-dimensional derivative : rolling moment due to sideslip

$\ell_\xi = \dfrac{\partial C_\ell}{\partial \xi}$ non-dimensional aileron power derivative

$\ell_p = \dfrac{\partial C_\ell}{\partial \frac{pb}{2V}}$ non-dimensional damping in roll derivative

M pitching moment

$M_\alpha = \dfrac{\partial M}{\partial \alpha}$ static longitudinal stability

$M_{\dot\alpha} = \dfrac{\partial M}{\partial \dot\alpha}$, $M_q = \dfrac{\partial M}{\partial q}$ pitch damping terms

$M_\eta = \dfrac{\partial M}{\partial \eta}$ elevator power

m aircraft mass

LIST OF SYMBOLS (Contd)

$m_w = \frac{\partial C_m}{\partial \alpha} \frac{c}{2\ell}$ non-dimensional pitch stability derivative

$m_\eta = \frac{\partial C_m}{\partial \eta} \frac{c}{2\ell}$ non-dimensional elevator power derivative

N yawing moment

$N_\beta = \frac{\partial N}{\partial \beta}$ directional stability

$N_r = \frac{\partial N}{\partial r}$ damping in yaw

$N_p = \frac{\partial N}{\partial p}$ yawing moment due to rate of roll

$N_\zeta = \frac{\partial N}{\partial \zeta}$ rudder power

$N_\xi = \frac{\partial N}{\partial \xi}$ yawing moment due to aileron

$n_v = \frac{\partial C_n}{\partial \beta}$ non-dimensional directional stability derivative

$n_\zeta = \frac{\partial C_n}{\partial \zeta}$ non-dimensional rudder power derivative

n load factor

p rate of roll

q rate of pitch

r rate of yaw

S wing area

t time

t_p pilot's time delay in control application

T_ψ period of directional oscillation

T_θ period of pitching oscillation

V speed

V_i equivalent airspeed

W weight

X tangential force

Y sideforce

$Y_\beta = \frac{\partial Y}{\partial \beta}$ sideforce due to sideslip

Z normal force

$Z_\alpha = \frac{\partial Z}{\partial \alpha}$ normal force due to incidence $\approx$ - lift slope

α incidence

β sideslip

λ root of stability equation

ϕ angle of bank

ζ rudder angle

ζ_D damping ratio of oscillatory motion

ξ aileron angle

η elevator angle

ω_e angular velocity of engine

$\omega_\psi = \frac{2\pi}{T_\psi}$ angular frequency of directional oscillation

$\omega_\theta = \frac{2\pi}{T_\theta}$ angular frequency of pitching oscillation

$\mu_2 = \frac{m}{\rho S b/2}$ relative density

APPENDIX I

The stability of the rolling aircraft with inertia cross-coupling

Neglecting gravity and minor aerodynamic terms in the force equations and assuming constant speed the aircraft motion is described by the five simultaneous differential equations:

$$\dot{\beta} = p\,(\alpha_o+\Delta\alpha) - r + \frac{1}{mV} Y_\beta\,\beta \qquad (I.1)$$

$$\dot{\alpha} = -p\beta + q + \frac{1}{mV} Z_\alpha \Delta\alpha \qquad (I.2)$$

$$\dot{p} = \frac{B-C}{A} qr + \frac{L_\zeta}{A}\zeta + \frac{L_\beta}{A}\beta + \frac{L_p}{A} p + \frac{L_r}{A} r \qquad (I.3)$$

$$\dot{q} = \frac{C-A}{B} rp + \frac{M_\eta}{B}\eta + \frac{M_\alpha}{B}\Delta\alpha + \frac{M_{\dot{\alpha}}}{B}\dot{\alpha} + \frac{M_q}{B} q \qquad (I.4)$$

$$\dot{r} = \frac{A-B}{C} pq + \frac{N_\zeta}{C}\zeta + \frac{N_\zeta}{C}\zeta + \frac{N_\beta}{C}\beta + \frac{N_p}{C} p + \frac{N_r}{C} r\,. \qquad (I.5)$$

Assuming constant rate of roll $p = p_o$ the rolling moment equation (I.3) becomes redundant and if rudder ζ and elevator η are assumed fixed the remaining equations are reduced to

$$\omega_\psi^2\,\beta + \frac{N_r}{C} - \frac{B-A}{B+A} q\,p_o - \dot{r} = -\frac{N_p}{C} p_o \qquad (I.6)$$

$$-\omega_\theta^2\,\Delta\alpha + \frac{M_q}{B} q + \frac{M_{\dot{\alpha}}}{B}\dot{\alpha} + p_o - \dot{q} = 0 \qquad (I.7)$$

$$\frac{Y_\beta}{mV}\beta + p_o\,\Delta\alpha - r - \dot{\beta} = p_o\,\alpha_o \qquad (I.8)$$

$$\frac{Z_\alpha}{mV}\Delta\alpha - p_o\,\beta + q - \dot{\alpha} = 0\,. \qquad (I.9)$$

In these equations it is assumed that approximately

$$C = A + B \qquad (I.10)$$

and the aerodynamic restoring moment is expressed by the frequencies: $\omega_\psi = \sqrt{N_\beta/C}$ and $\omega_\theta = \sqrt{-M_\alpha/B}$. If aerodynamic damping terms are neglected, the characteristic equation will reduce to a biquadratic in $\left(\frac{\lambda}{p_o}\right)$:

$$\left(\frac{\lambda}{p_o}\right)^2 = -\frac{1}{2}\left\{\left(\frac{\omega_\psi}{p_o}\right)^2 + \left(\frac{\omega_\theta}{p_o}\right)^2 + 1 + \frac{B-A}{B+A}\right\}$$

$$\pm\sqrt{\frac{1}{4}\left\{\left(\frac{\omega_\psi}{p_o}\right)^2 + \left(\frac{\omega_\theta}{p_o}\right)^2 + 1 + \frac{B-A}{B+A}\right\}^2 - \left(\frac{\omega_\psi}{p_o}\right)^2\left(\frac{\omega_\theta}{p_o}\right)^2 + \left(\frac{\omega_\psi}{p_o}\right)^2 - \frac{B-A}{B+A}\left\{1 - \left(\frac{\omega_\theta}{p_o}\right)^2\right\}}\,. \qquad (I.11)$$

APPENDIX II

Autorotational rolling

Assuming steady rolling with

$$\dot{p} = \dot{r} = \dot{q} = \dot{\alpha} = \dot{\beta} = 0$$

and

$$p = \text{const}; \quad r = \text{const}; \quad q = \text{const}; \quad \alpha = \text{const}; \quad \beta = \text{const}$$

equations (I.1)-(I.5) are reduced to

$$L_\beta \beta + L_p p = 0 \tag{II.1}$$

$$N_\beta \beta - pq (B-A) = 0 \tag{II.2}$$

$$M_\alpha \alpha - M_q q + pr B = 0 \tag{II.3}$$

$$\frac{Z_\alpha}{mV} \alpha + q - p\beta = 0 \tag{II.4}$$

$$- r + p (\alpha+\alpha_o) = 0 . \tag{II.5}$$

These equations give a biquadratic in p, the real solutions of which describe two equilibrium rolling states

$$\left(\frac{p}{\omega_{\psi_o}}\right)^2 = \frac{1}{2}\left\{1 + \left(\frac{\omega_\theta}{\omega_{\psi_o}}\right)^2 + \alpha_o \nu\right\} \pm \sqrt{\frac{1}{4}\left\{1 + \left(\frac{\omega_\theta}{\omega_{\psi_o}}\right)^2 + \alpha_o \nu\right\}^2 - \left(\frac{\omega_\theta}{\omega_{\psi_o}}\right)^2 - \kappa} \qquad \ldots\ldots \text{(II.6)}$$

with

$$\omega_{\psi_o} = \omega_\psi \left(\frac{B+A}{B-A}\right)$$

$$\nu = z_w \frac{\ell_v}{\ell_p} \frac{i_C - 2i_A}{n_v}$$

$$\kappa = z_w \frac{m_q}{n_v}\left(1 - \frac{A}{B}\right) \frac{\left(\frac{\ell}{b/2}\right)^2}{\mu_2} .$$

Co-ordinated values for the other variables of motion as applicable to the steady rolling states can be obtained from equations (II.1)-(II.6):

$$\alpha = \frac{1 - \left(\frac{p}{\omega_{\psi_o}}\right)^2}{\nu} \qquad \beta = - p \frac{\ell_p}{\ell_v} \frac{b/2}{V}$$

$$q = - \omega_{\psi_o}^2 \frac{\ell_p}{\ell_v} \frac{b/2}{V} \qquad r = p (\alpha_o+\alpha) . \tag{II.7}$$

APPENDIX III

Control required to prevent pitch and yaw building up in inertia-coupled rolling

Putting $\Delta\alpha = \beta = 0$ and assuming a given rolling manoeuvre as $p(t)$ and thus $\dot{p}(t) = \frac{d\,p(t)}{dt}$, equations (I.1)-(I.5) are reduced to

$$L_\xi\,\xi + L_p\,p - A\,\dot{p} = 0 \qquad \text{(III.1)}$$

$$N_\xi\,\xi + N_\zeta\,\zeta + N_p\,p + N_r\,\alpha_o\,p - C\,\dot{p}\,\alpha_o = 0 \qquad \text{(III.2)}$$

$$M_\eta\,\eta + (C-A)\,p^2\,\alpha_o = 0\,. \qquad \text{(III.3)}$$

These equations can now be solved for the control angles:

$$\xi(t) = \frac{A}{L_\xi}\,\dot{p}(t) - \frac{L_p}{L_\xi}\,p(t) \qquad \text{(III.4)}$$

$$\zeta(t) = \frac{C}{N_\zeta}\,\alpha_o\,\dot{p}(t) - \left(\frac{N_p}{N_\zeta} + \alpha_o\,\frac{N_r}{N_\zeta}\right)p(t) - \frac{N_\xi}{N_\zeta}\,\xi(t) \qquad \text{(III.5)}$$

$$\eta(t) = -\frac{C-A}{M_\eta}\,\alpha_o\,p^2(t)\,. \qquad \text{(III.6)}$$

APPENDIX IV

Pitch up response with pilot's counter control

Representing the aircraft motion in pitch by the one degree of freedom approximation

$$\frac{M_\alpha}{B}\Delta\alpha + \frac{M_{\dot\theta}}{B} q - \dot q = -\frac{M_\eta}{B}\eta \qquad \text{(IV.1)}$$

where $q = \frac{d\alpha}{dt}$, and $\frac{M_{\dot\theta}}{B}$ is an equivalent total damping in pitch

$$\frac{M_{\dot\theta}}{B} = \frac{M_q}{B} + \frac{M_{\dot\alpha}}{B} + Z_\alpha \,. \qquad \text{(IV.2)}$$

The roots of the characteristic equation for this system are

$$\lambda = +\frac{M_{\dot\theta}}{B}\frac{1}{2} \pm \sqrt{\frac{1}{4}\left(\frac{M_{\dot\theta}}{B}\right)^2 - \frac{M_\alpha}{B}} \qquad \text{(IV.3)}$$

as plotted in Fig.26.

Assuming the aircraft to be initially in steady flight i.e. at $t = 0$: $\Delta\alpha = \dot\alpha = 0$, the motion resulting from a disturbance in elevator $\eta = \eta_o$ for $0 < t < t_P$ is described by

$$\Delta\alpha = \alpha_1 e^{\lambda_1 t} + \alpha_2 e^{\lambda_2 t} + \alpha_o \qquad \text{(IV.4)}$$

where from equation (IV.1)

$$\alpha_o = -\eta_o \frac{m_\eta}{m_w} \qquad \text{(IV.5)}$$

from $\dot\alpha = \alpha_1\lambda_1 e^{\lambda_1 t} + \alpha_2 e^{\lambda_2 t}$ and the initial conditions:

$$\alpha_1 = -\frac{\alpha_o}{1 - \frac{\lambda_1}{\lambda_2}}\,; \qquad \alpha_2 = -\frac{\alpha_o}{1 - \frac{\lambda_2}{\lambda_1}}\,. \qquad \text{(IV.6)}$$

Thus after t_P seconds

$$\Delta\alpha = -\frac{\alpha_o}{1 - \frac{\lambda_1}{\lambda_2}} e^{\lambda_1 t_P} - \frac{\alpha_o}{1 - \frac{\lambda_2}{\lambda_1}} e^{\lambda_2 t_P} + \alpha_o \qquad \text{(IV.7)}$$

$$\dot\alpha = -\lambda_1 \frac{\alpha_o}{1 - \frac{\lambda_1}{\lambda_2}} e^{\lambda_1 t_P} - \lambda_2 \frac{\alpha_o}{1 - \frac{\lambda_2}{\lambda_1}} e^{\lambda_2 t_P}\,. \qquad \text{(IV.8)}$$

At t_P the pilot applies counter elevator $\eta = \eta_R$ and using $t^* = t - t_P$ we get for $t > t_P$ the aircraft response as:

$$\Delta\alpha = A_1 e^{\lambda_1 t^*} + A_2 e^{\lambda_2 t^*} + \alpha_S \qquad \text{(IV.9)}$$

$$\dot{\alpha} = \lambda_1 A_1 e^{\lambda_1 t^*} + \lambda_2 A_2 e^{\lambda_2 t^*} . \qquad \text{(IV.10)}$$

From equation (IV.1) the "trimmed incidence"

$$\alpha_S = -\eta_R \frac{m_\eta}{m_w} . \qquad \text{(IV.11)}$$

Substituting the expressions (IV.4) and (IV.5) as initial conditions into equations (IV.9)-(IV.10) we get

$$\frac{A_1}{\alpha_S} = -\frac{1 - \frac{\alpha_o}{\alpha_S}\left(1 - e^{\lambda_1 t_P}\right)}{1 - \frac{\lambda_1}{\lambda_2}} \qquad \text{(IV.12)}$$

$$\frac{A_2}{\alpha_S} = -\frac{1 - \frac{\alpha_o}{\alpha_S}\left(1 - e^{\lambda_1 t_P}\right)}{1 - \frac{\lambda_2}{\lambda_1}} . \qquad \text{(IV.13)}$$

The maximum overswing amplitude in $\Delta\alpha$ occurs for $\dot{\alpha} = 0$ at t_m^* which can be obtained by putting in equation (IV.10) $\dot{\alpha} = 0$ to give

$$e^{t_m^*(\lambda_1 - \lambda_2)} = \frac{1 - \frac{\alpha_o}{\alpha_S}\left(1 - e^{\lambda_2 t_P}\right)}{1 - \frac{\alpha_o}{\alpha_S}\left(1 - e^{\lambda_1 t_P}\right)}$$

or

$$t_m^* \lambda_1 = \frac{1}{1 - \frac{\lambda_2}{\lambda_1}} \ell n \frac{1 - \frac{\alpha_o}{\alpha_S}\left(1 - e^{\lambda_2 t_P}\right)}{1 - \frac{\alpha_o}{\alpha_S}\left(1 - e^{\lambda_1 t_P}\right)} . \qquad \text{(IV.14)}$$

Thus the peak overshoot in $\Delta\alpha$ is now obtained as

$$\frac{\Delta\alpha_{max}}{\alpha_S} = 1 + \frac{A_1}{\alpha_S} e^{\lambda_1 t_m^*} + \frac{A_2}{\alpha_S} e^{\lambda_2 t_m^*} . \qquad \text{(IV.15)}$$

These values have been computed for a representative range of the parameters $\lambda_1 t_P$, $\alpha_S/\alpha_o = \eta_R/\eta_o$ and for two ratios $\lambda_2/\lambda_1 = -1$ and $\lambda_2/\lambda_1 = -2$. Results are plotted in Fig.29.

APPENDIX V

Aircraft response in self-stabilizing pitch up

Considering the pitching moment characteristic illustrated in Fig.30, the aircraft is again assumed to be initially trimmed for steady flight at an incidence α_K. Elevator η_o is then applied to induce nose up pitch and held until the motion dies down.

If $\Delta\alpha$ is the incremental incidence from the initial state, i.e. $\alpha = \alpha_K + \Delta\alpha$, within the unstable range the aircraft response is given by equations (IV.4)-(IV.6)

$$\frac{\Delta\alpha}{\alpha_o} = -\frac{e^{\lambda_1 t}}{1-\frac{\lambda_1}{\lambda_2}} - \frac{e^{\lambda_2 t}}{1-\frac{\lambda_2}{\lambda_1}} + 1 \qquad (V.1)$$

for not too small values of λ_2, λ_2 being the negative stable root, the second term on the right hand side becomes negligible after a short transient, this gives the instant when $\Delta\alpha = \alpha_u$, i.e. at the end of the unstable incidence range

$$\frac{e^{\lambda_1 t}}{1-\frac{\lambda_1}{\lambda_2}} \approx -\frac{\Delta\alpha}{\alpha_o} = \frac{\alpha_u}{\alpha_o}.$$

Substituted into equation (IV.8) we get

$$\frac{\dot{\alpha}}{\alpha_o} = \lambda_1 \frac{\alpha_u}{\alpha_o} \quad \text{or} \quad \dot{\alpha} = \lambda_1 \alpha_u . \qquad (V.2)$$

Thus values $\Delta\alpha = \alpha_u$ and $\dot{\alpha} = \lambda_1 \alpha_u$ can be used as initial conditions for the motion in the succeeding stable range beyond α_R

$$\Delta\alpha = \alpha_A (\omega_\theta t^* + \varepsilon)\, e^{\lambda_\theta t^*} \qquad (V.3)$$

$$\dot{\alpha} = \alpha_A \{\lambda_\theta \cos(\omega_\theta t^* + \varepsilon) - \omega_\theta \sin(\omega_\theta t^* + \varepsilon)\}\, e^{\lambda_\theta t^*} . \qquad (V.4)$$

These equations are again solved for the maximum in $\Delta\alpha$. From the initial conditions we get

$$\frac{\alpha_A}{\alpha_S} = \sqrt{1 + \left(\frac{\alpha_u}{\alpha_S}\frac{\lambda_1}{\omega_\theta} - \zeta_D\right)} \qquad (V.5)$$

and

$$\cos\varepsilon = \frac{\alpha_S}{\alpha_A} \qquad (V.6)$$

where $\zeta_D = -\frac{\lambda_\theta}{\omega_\theta}$, the damping ratio of the oscillation.

Putting $\dot{\alpha} = 0$ in equation (V.4) we get

$$\omega_\theta t_m = 2\pi - \varepsilon_D - \sin^{-1} \zeta_D \,. \qquad (V.7)$$

The peak overshoot amplitude is then given by

$$\frac{\Delta\alpha_{max}}{\alpha_S} = \frac{\alpha_A}{\alpha_S} \sqrt{1 - \zeta_D^2}\; e^{-\zeta_D(2\pi - \varepsilon_D - \sin^{-1}\zeta_D)} \,. \qquad (V.8)$$

WT.2078.C.P.404.K3 - Printed in Great Britain

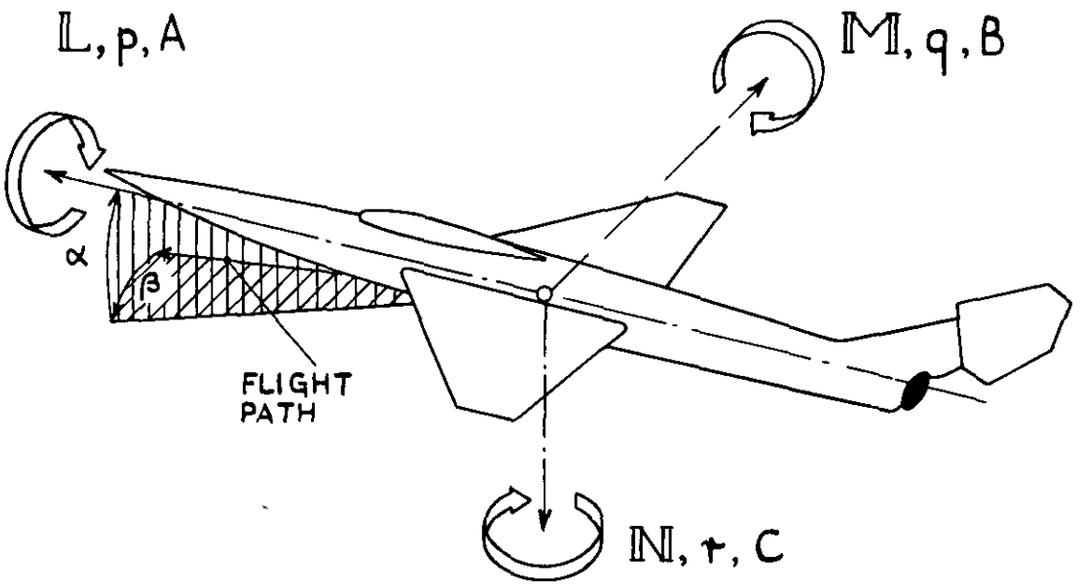

FIG.1. SYSTEM OF AXES USED IN THE ANALYSIS OF INERTIA CROSSCOUPLING PHENOMENA.

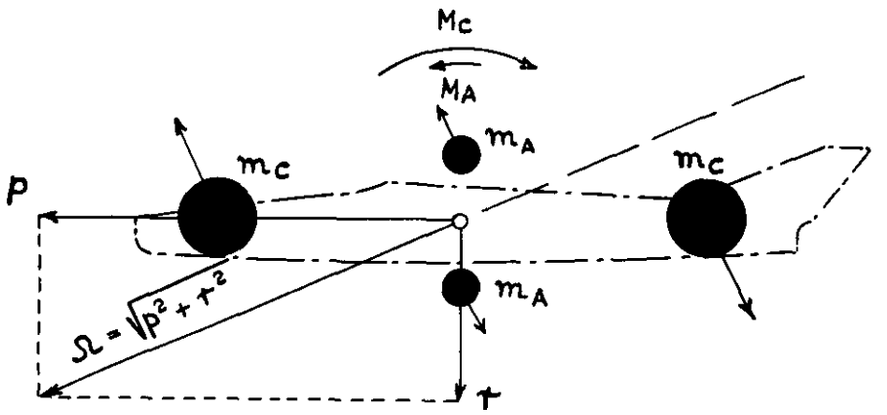

FIG.2. THE GYROSCOPIC MOMENT $M = pr\,(C-A)$

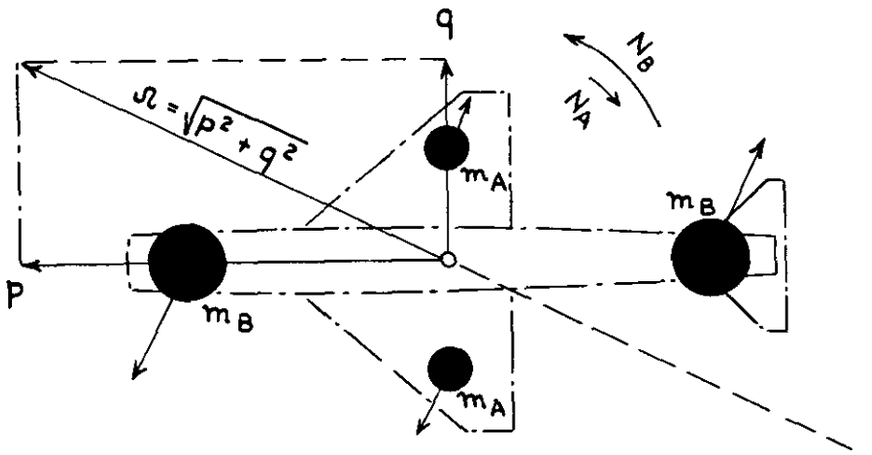

FIG.3 THE GYROSCOPIC MOMENT $N = p\,q\,(A-B)$

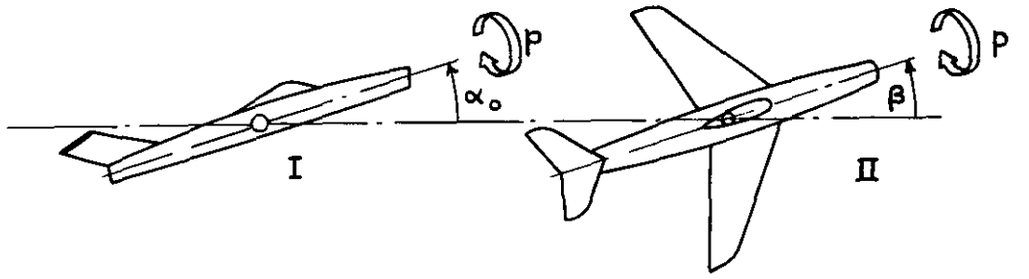

FIG.4. THE KINEMATIC TERM $p\alpha = \dot{\beta}$

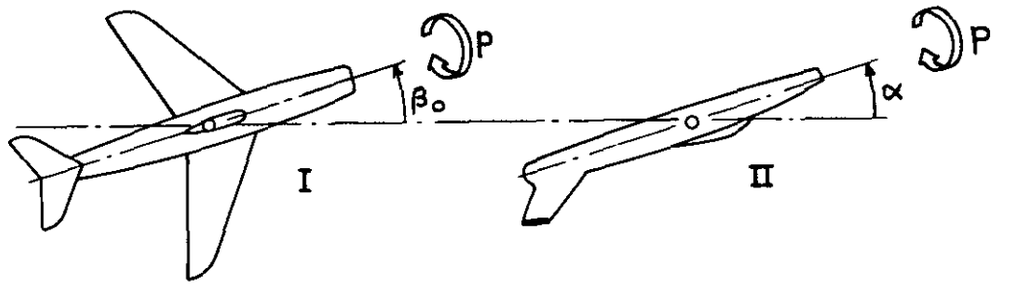

FIG 5. THE KINEMATIC TERM $p\beta = -\dot{\alpha}$

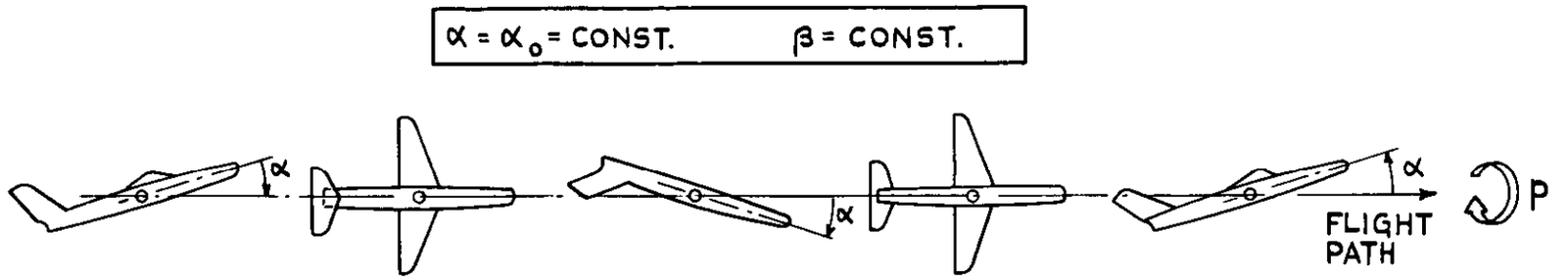

FIG. 6. STABLE ROLLING OF AN AIRCRAFT WITH INFINITELY LARGE STABILITY IN PITCH AND YAW OR NEGLEGIBLE INERTIAS.

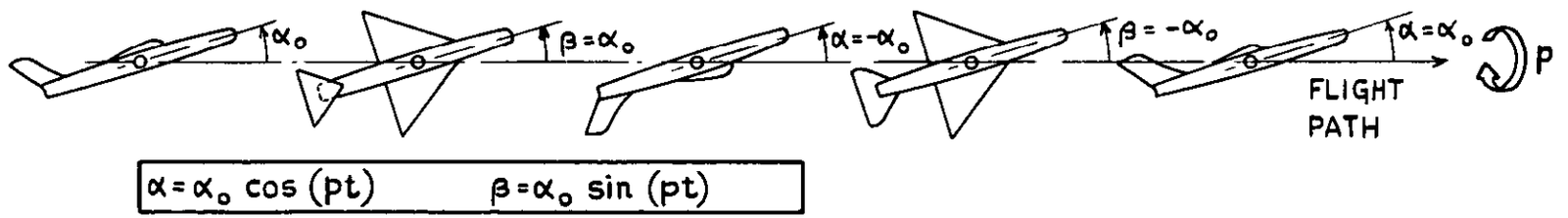

FIG. 7. STABLE ROLLING OF AN AIRCRAFT WITH INFINITELY LARGE INERTIA OR NEGLEGIBLE STABILITIES. PITCH AND YAW ARE PERIODIC.

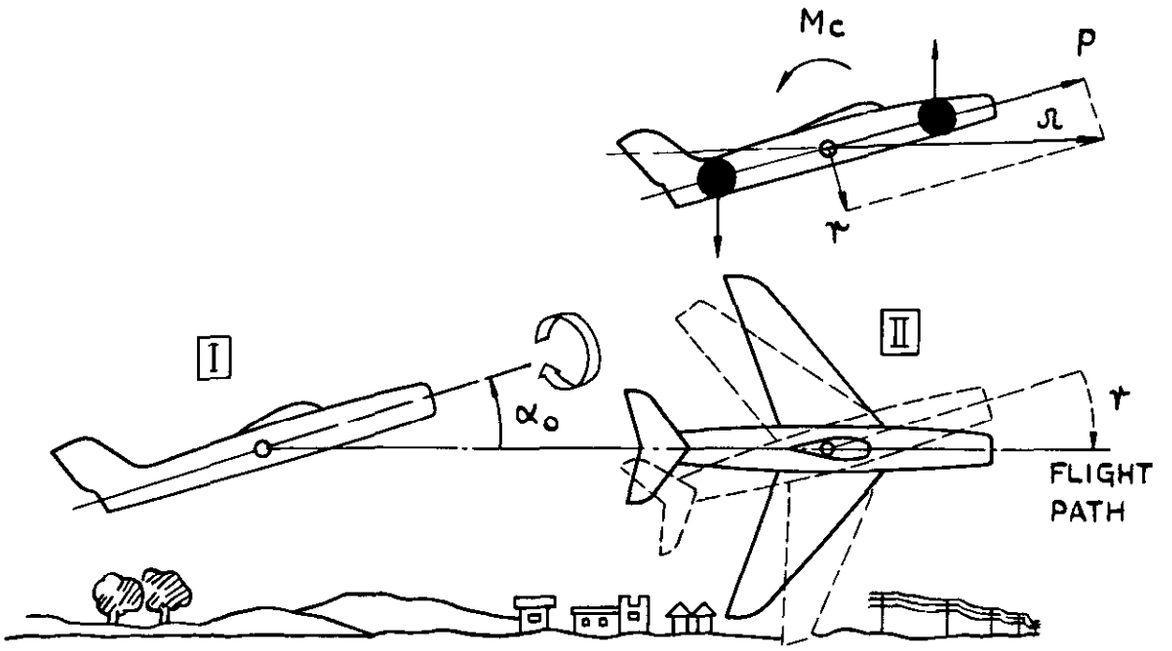

FIG.8. YAWING INERTIA COUPLE LEADING TO PITCH DIVERGENCE IF m_w IS INSUFFICIENT.

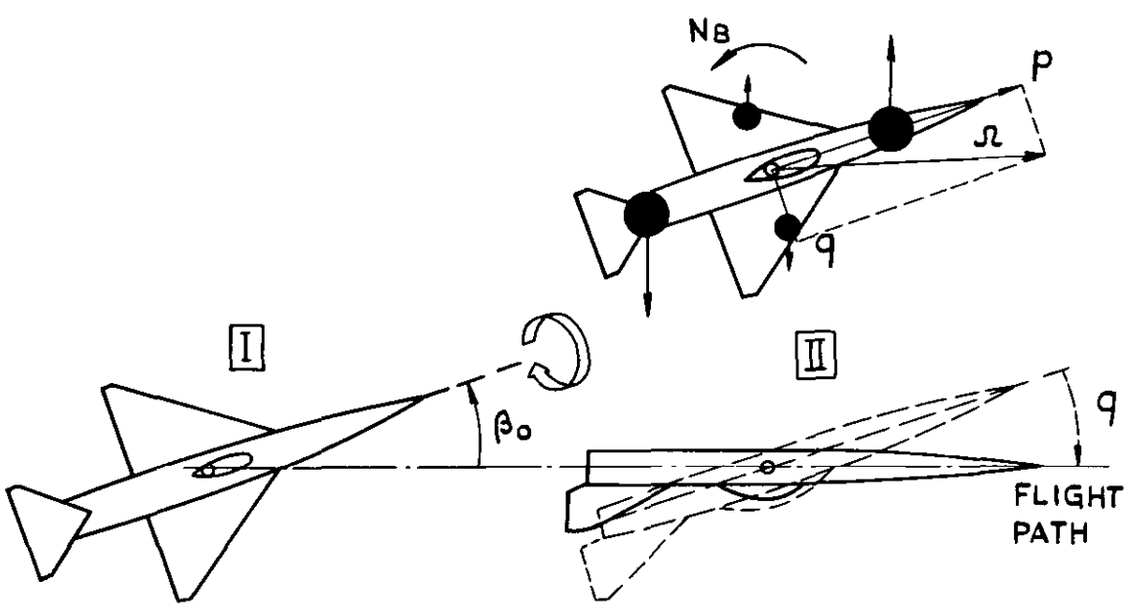

FIG.9. PITCHING INERTIA COUPLE LEADING TO YAW-DIVERGENCE IF n_v IS INSUFFICIENT.

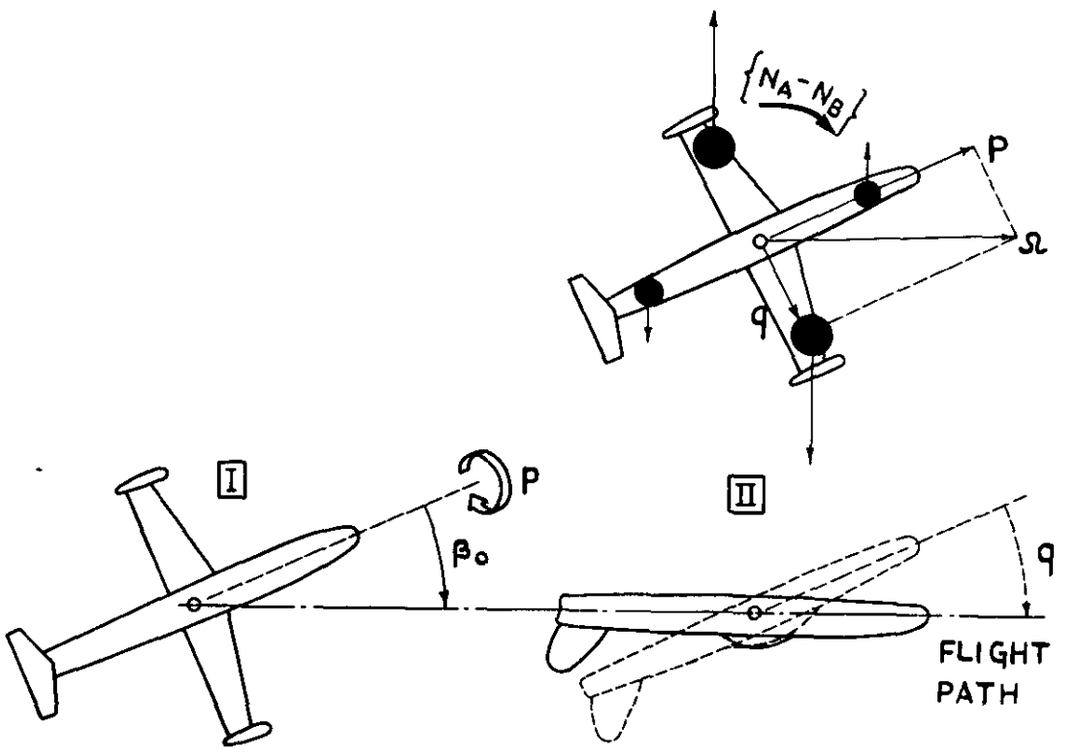

FIG.10. ROLLING INERTIA COUPLE STABILIZING AGAINST PITCHING INERTIA COUPLE

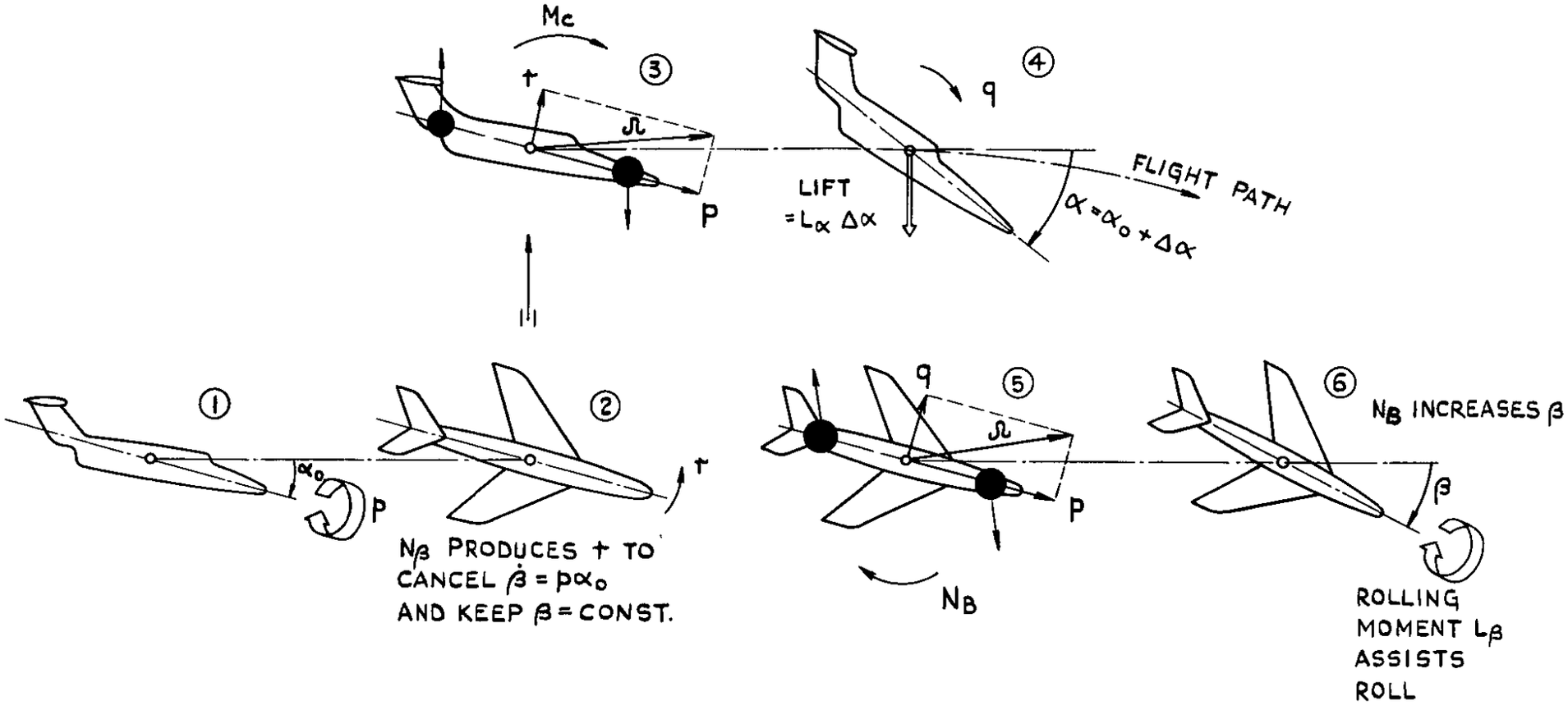

FIG.11. AUTOROTATION IN ROLL RESULTING FROM INERTIA CROSSCOUPLING.

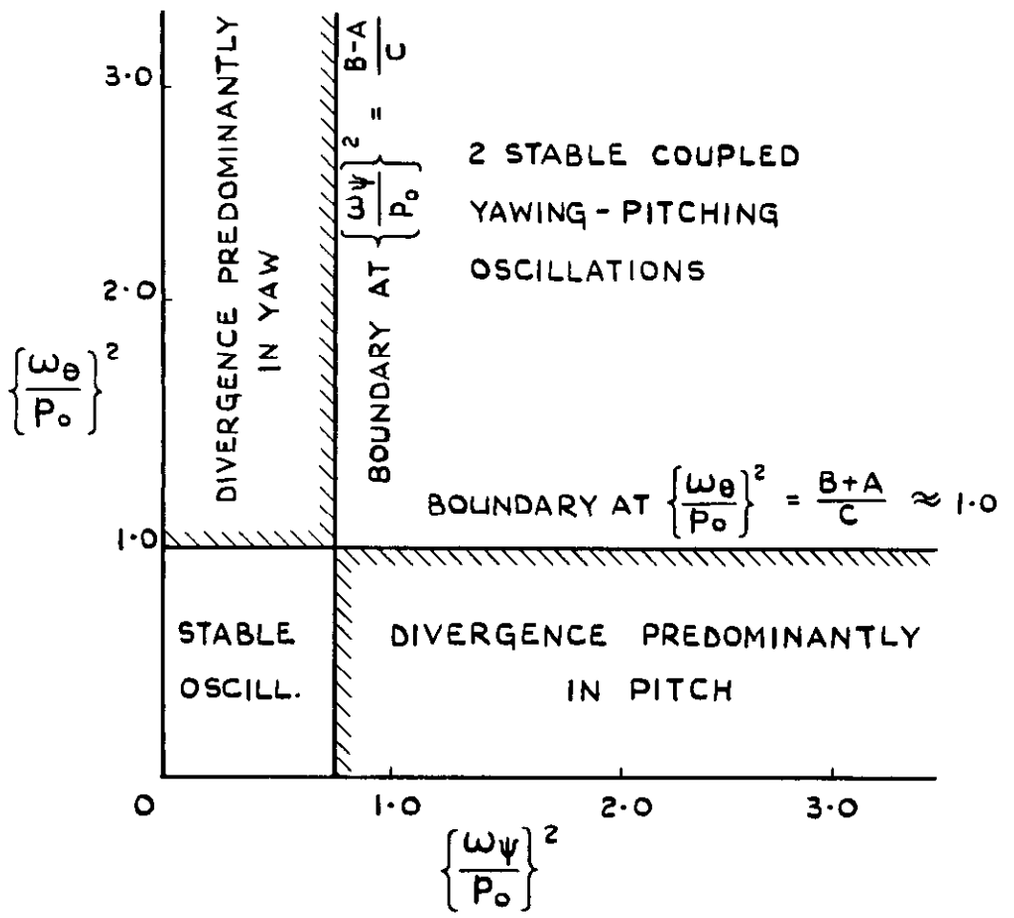

ω_θ = FREQUENCY OF UNCOUPLED PITCHING - OSCILLATION

ω_ψ = FREQUENCY OF UNCOUPLED LATERAL - OSCILLATION

p_o = STEADY RATE OF ROLL IN RAD/SEC.

A = INERTIA IN ROLL

B = INERTIA IN PITCH.

C = INERTIA IN YAW.

FIG.12. STABILITY DIAGRAM FOR THE ROLLING AIRCRAFT ACCORDING TO PHILLIPS.

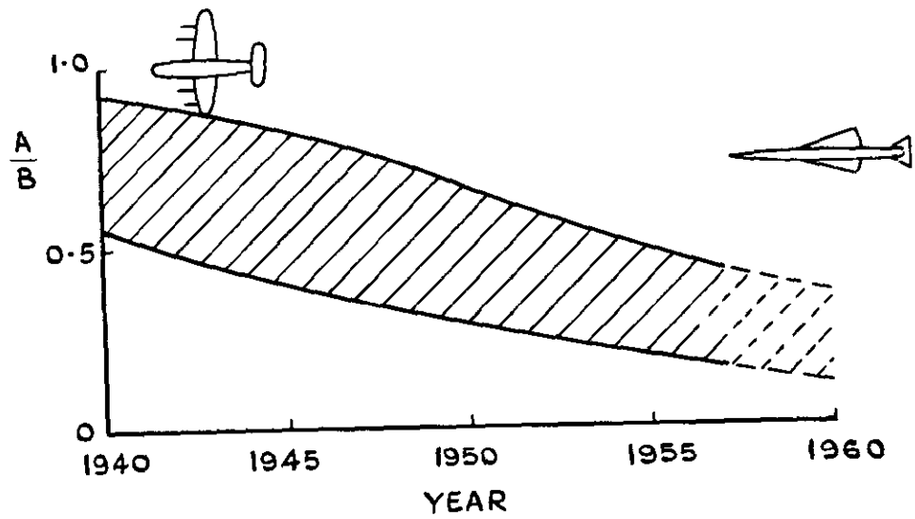

FIG.13. TRENDS IN INERTIA DISTRIBUTION BETWEEN ROLL (A) AND PITCH (B)

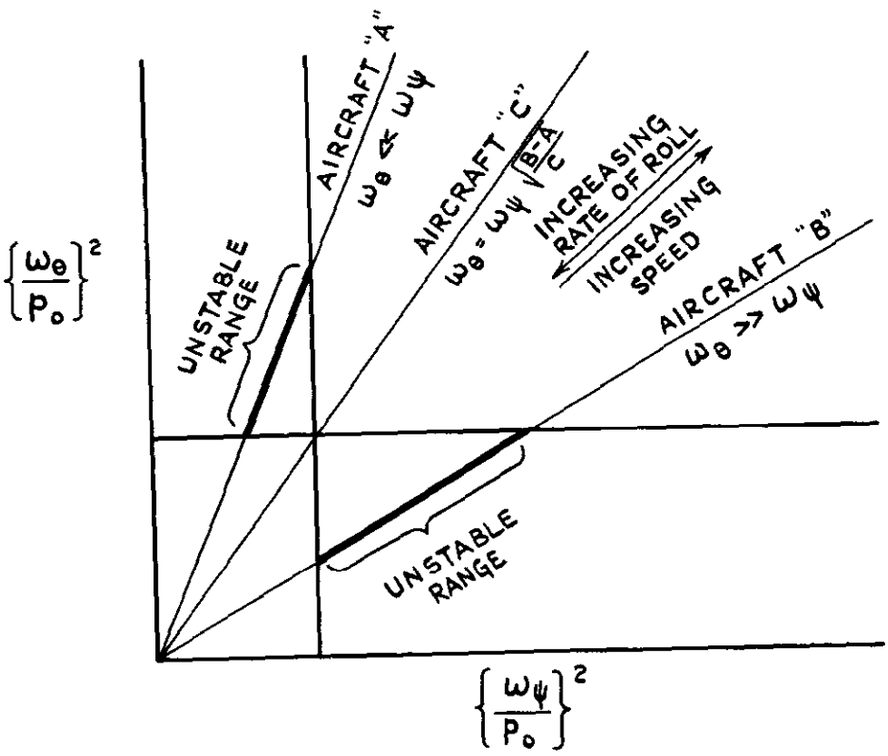

FIG.14. THE EFFECT OF INERTIA CROSSCOUPLING ON THREE AIRCRAFT CONFIGURATIONS.

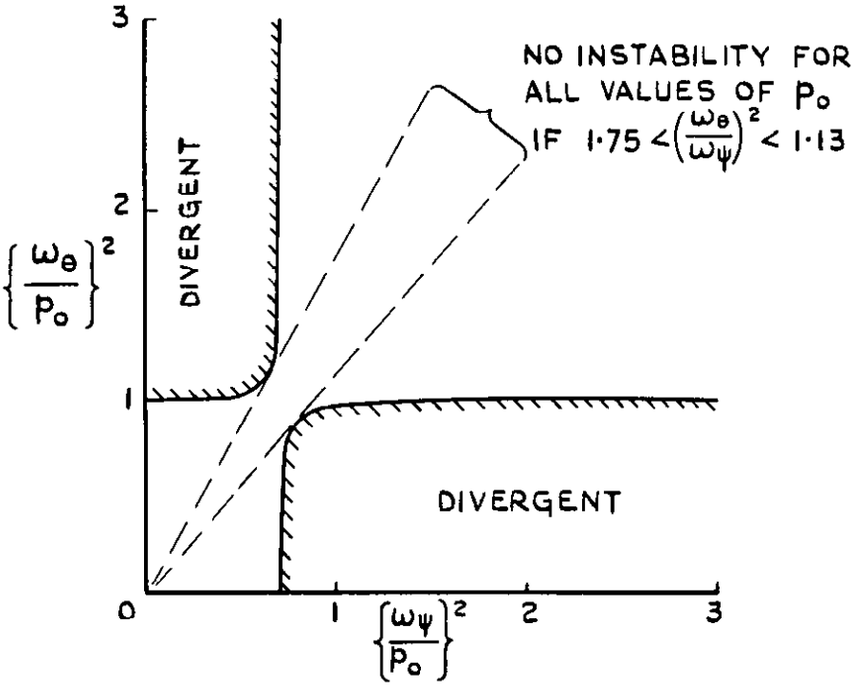

FIG.15. EFFECT OF DAMPING IN YAW AND PITCH ON THE DIVERGENCE BOUNDARIES.

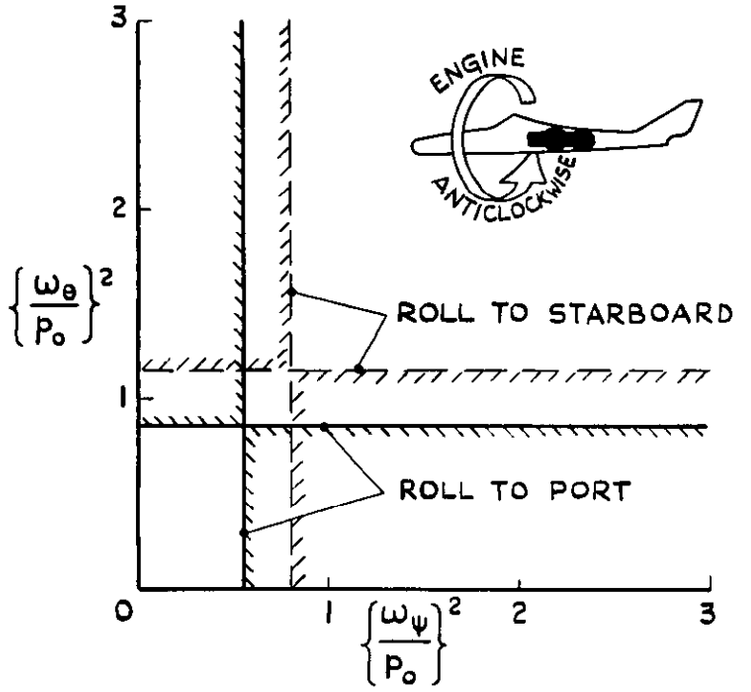

FIG.16. EFFECT OF ENGINE MOMENTUM ON THE DIVERGENCE BOUNDARIES.

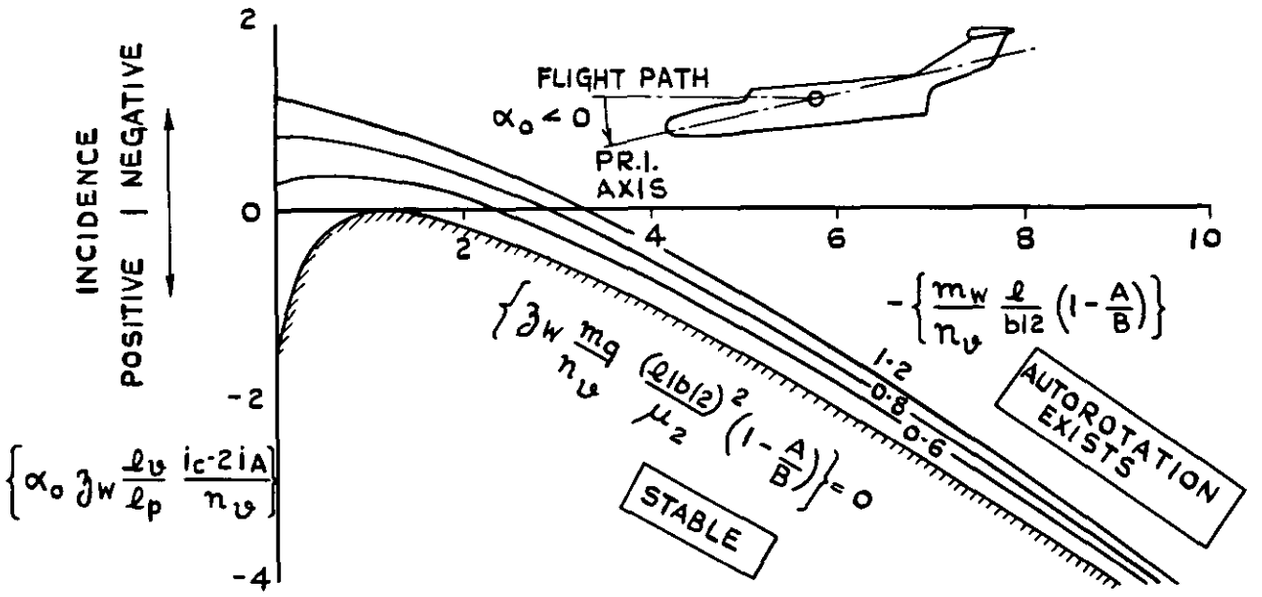

FIG.17. CRITICAL INCIDENCE α_0 BELOW WHICH AUTOROTATIONAL ROLLING EXISTS.

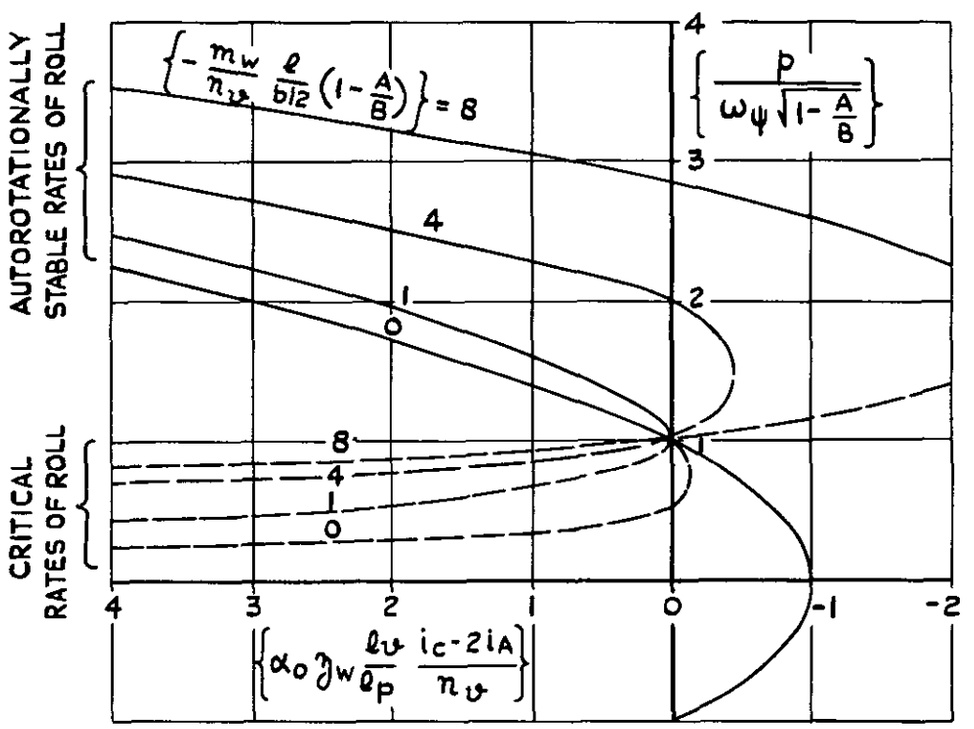

FIG.18. CRITICAL RATE OF ROLL FOR ROLL DIVERGENCE AND AUTOROTATIONAL RATE OF ROLL.

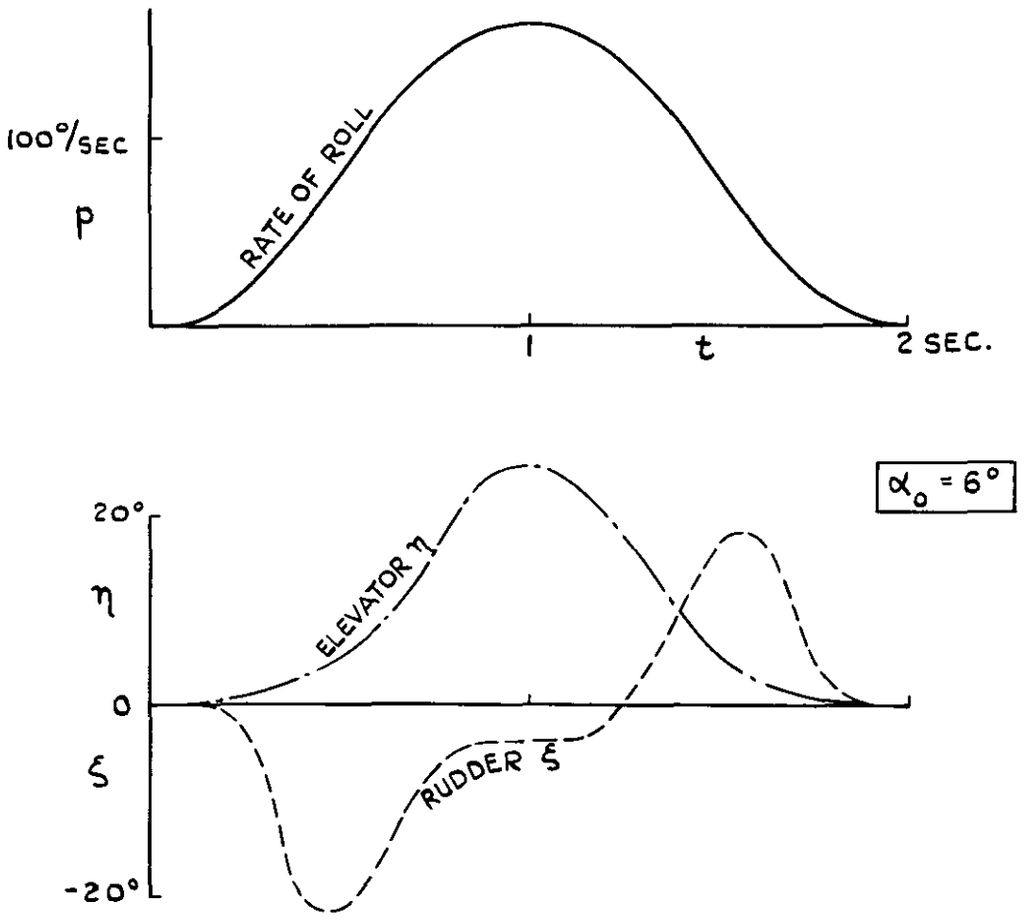

FIG. 19. ELEVATOR AND RUDDER ANGLES REQUIRED TO HOLD AN AIRCRAFT WITH INERTIA CROSSCOUPLING IN A BANK MANOEUVRE THROUGH 180°.

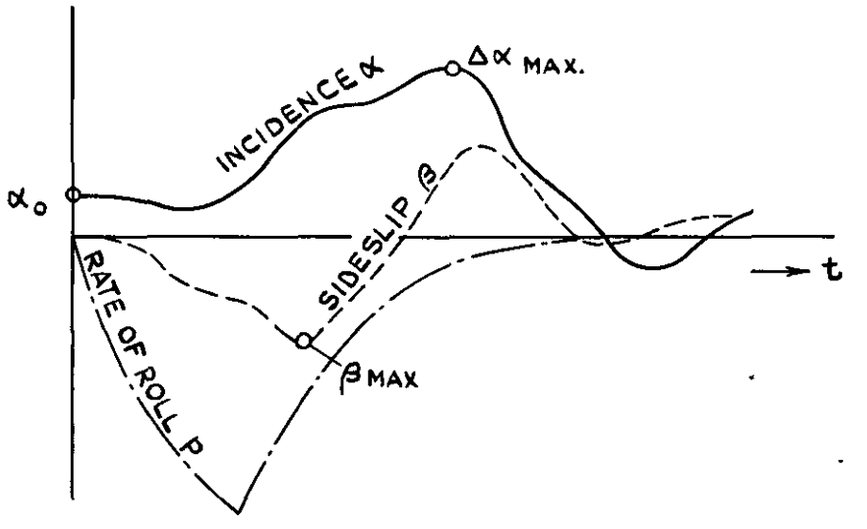

FIG. 20. TYPICAL TIME HISTORY OF INERTIACOUPLED ROLLING MANOEUVRE.

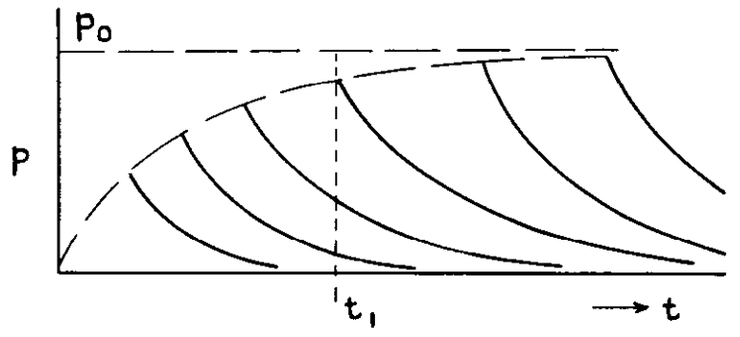

FIG. 21. FAMILY OF ROLLING MANOEUVRES USED IN THE COMPUTATIONS.

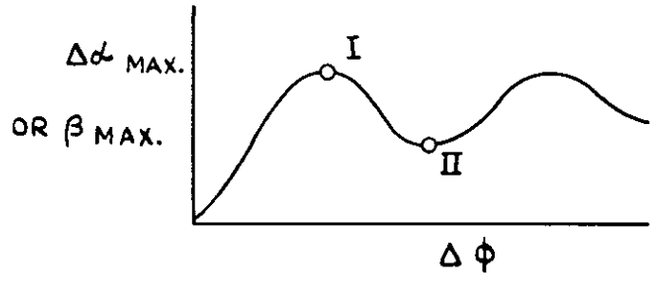

(a) STABLE CONDITION

$$p_o^2 < \omega_\theta^2$$

$$p_o^2 < \omega_\psi^2 \frac{B-A}{C}$$

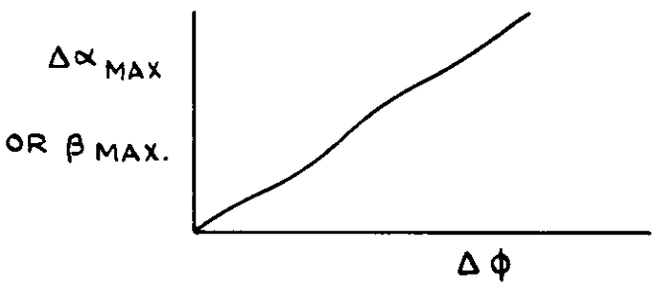

(b) NEUTRALLY STABLE

$$p_o^2 = \omega_\theta^2$$

OR $$p_o^2 = \omega_\psi^2 \frac{B-A}{C}$$

(c) DIVERGENT CONDITION

$$\omega_\theta^2 \lesssim p_o^2 \lesssim \omega_\psi^2 \frac{B-A}{C}$$

FIG. 22. (a-c) VARIATION OF PEAK LOADS IN INCIDENCE AND SIDESLIP WITH THE DURATION OF THE ROLLING MANOEUVRE.

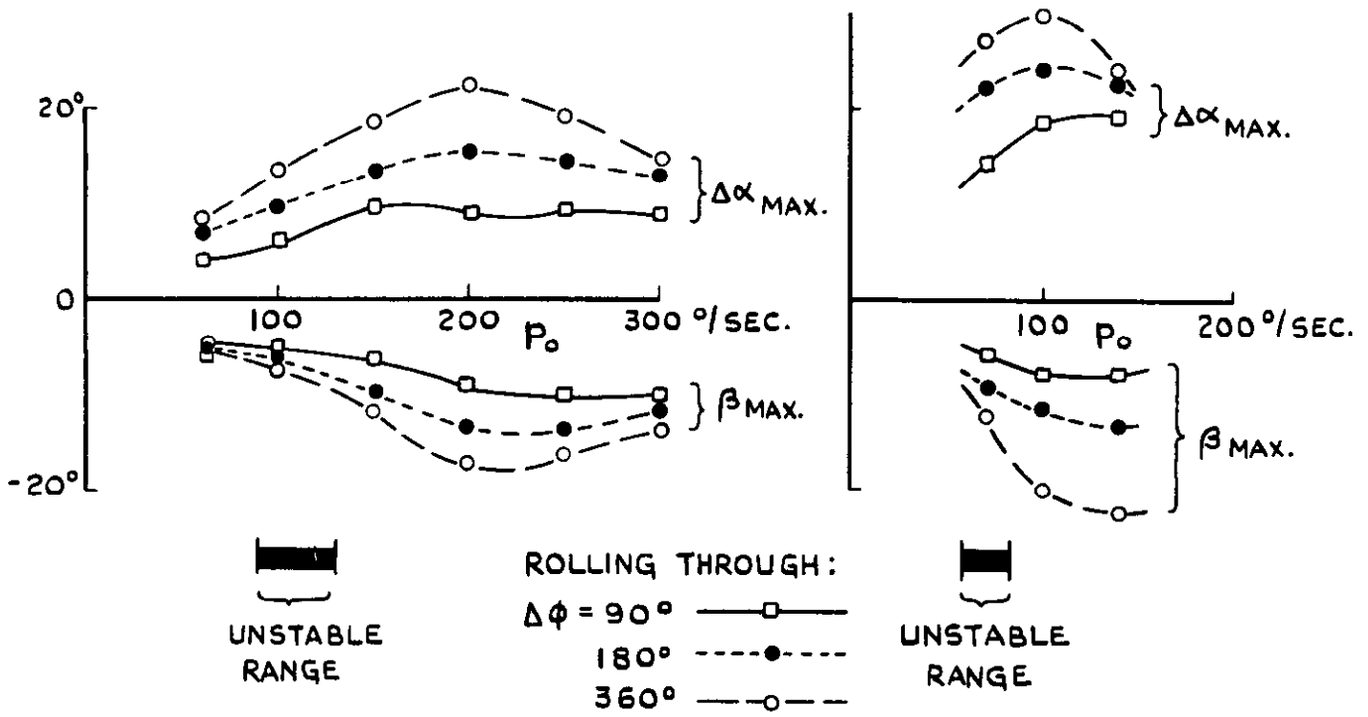

FIG. 23. EFFECT OF ROLLING VELOCITY ON THE PEAK VALUES IN INCIDENCE AND SIDESLIP.

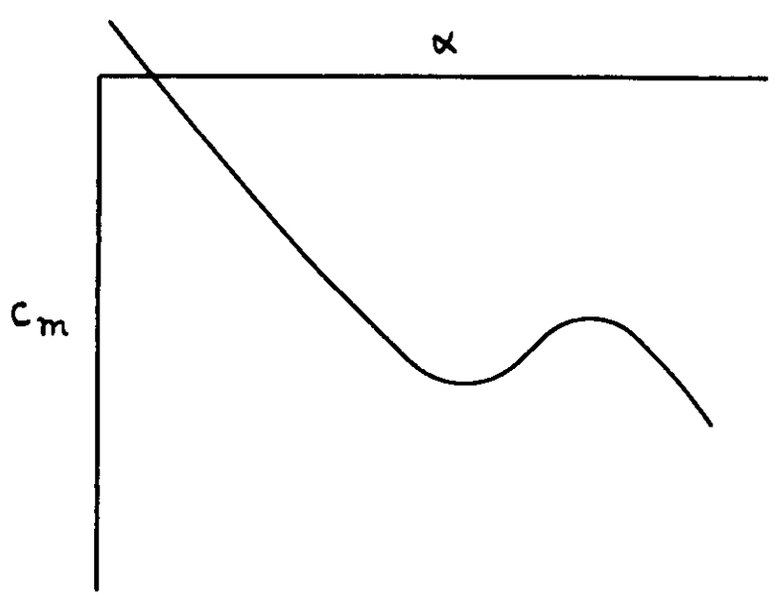

FIG. 24. TYPICAL EXAMPLE OF A PITCH UP CHARACTERISTIC.

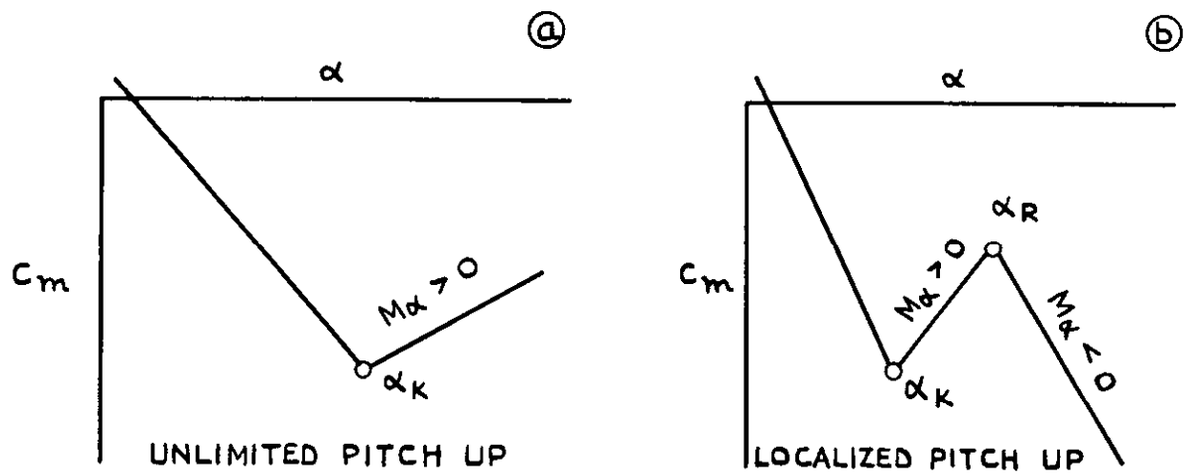

FIG. 25(a & b) SIMPLIFIED PITCH UP CHARACTERISTICS FOR NUMERICAL ANALYSIS.

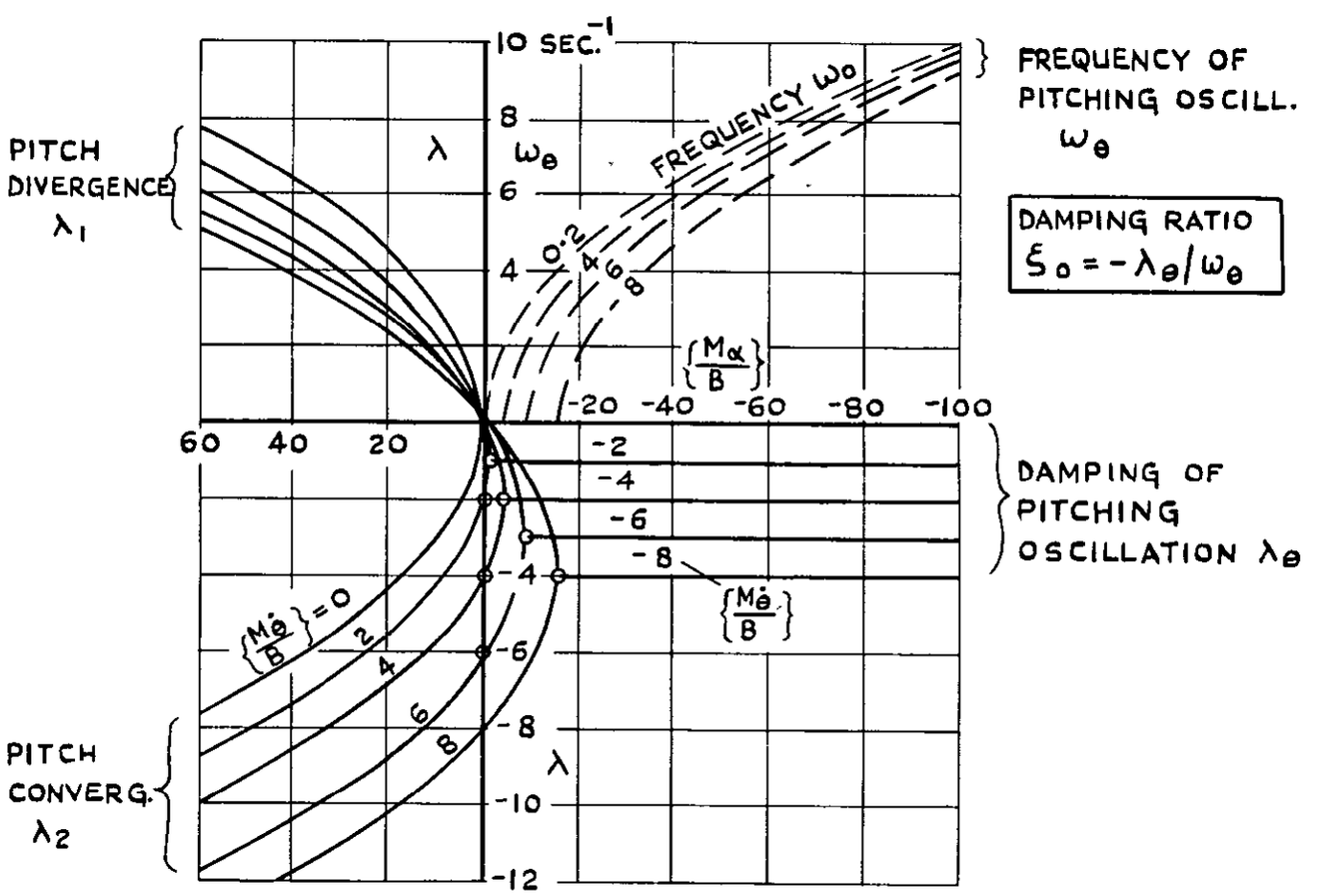

FIG. 26. ROOTS OF THE PITCHING MOTION FOR STABLE AND UNSTABLE STATIC STABILITY $M_\alpha = \vartheta_M / \vartheta_\alpha$.

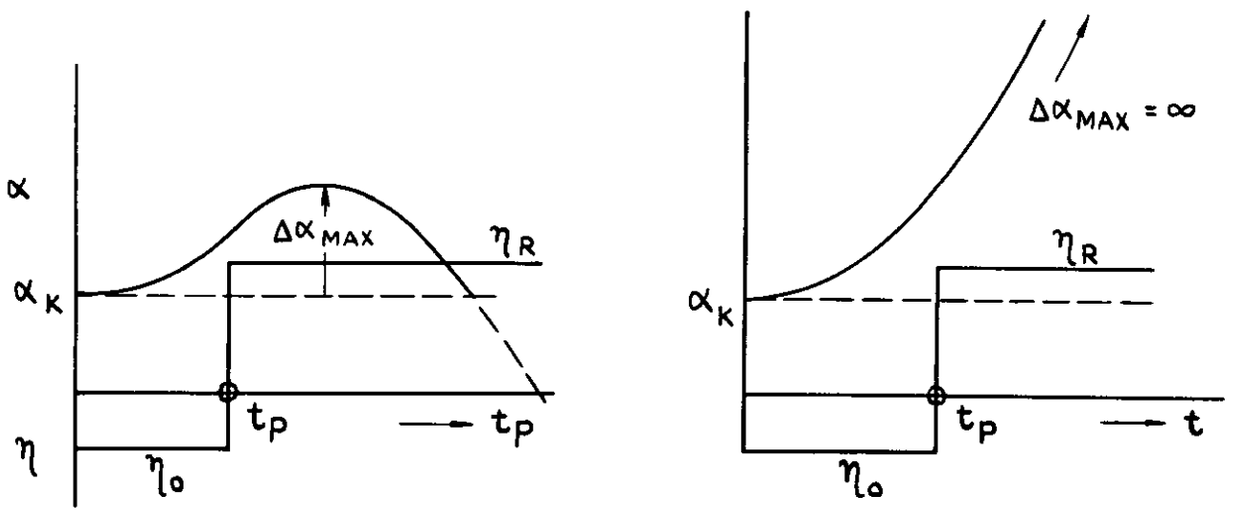

FIG. 27. TYPICAL TIME HISTORY OF A PITCH UP MANOEUVRE WITH ATTEMPTED RECOVERY BY THE PILOT.

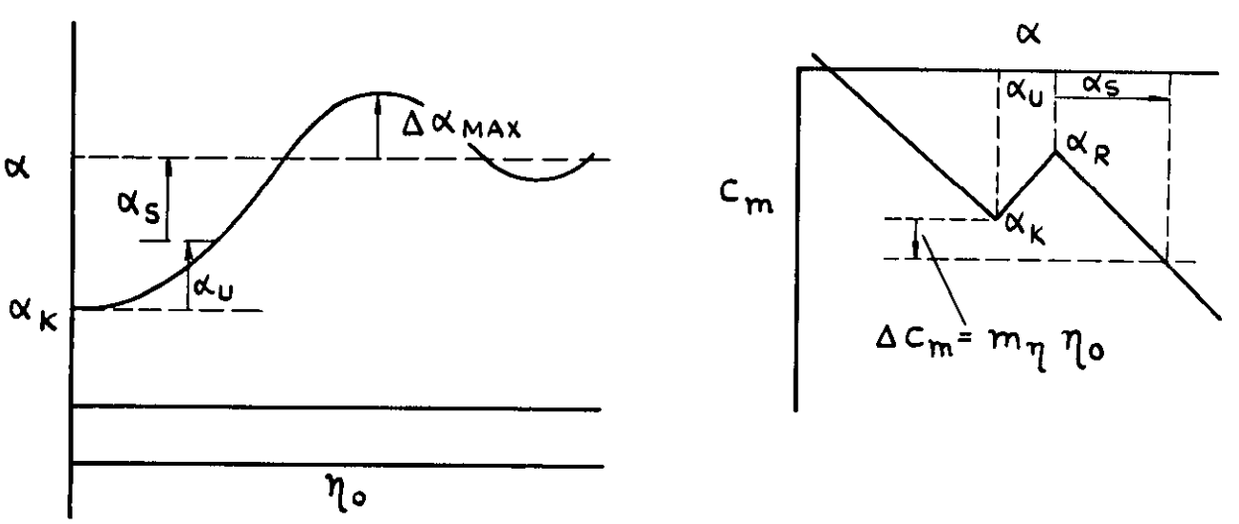

FIG. 28. TYPICAL TIME HISTORY OF AN UNCONTROLLED SELF STABILIZING PITCH UP MANOEUVRE.

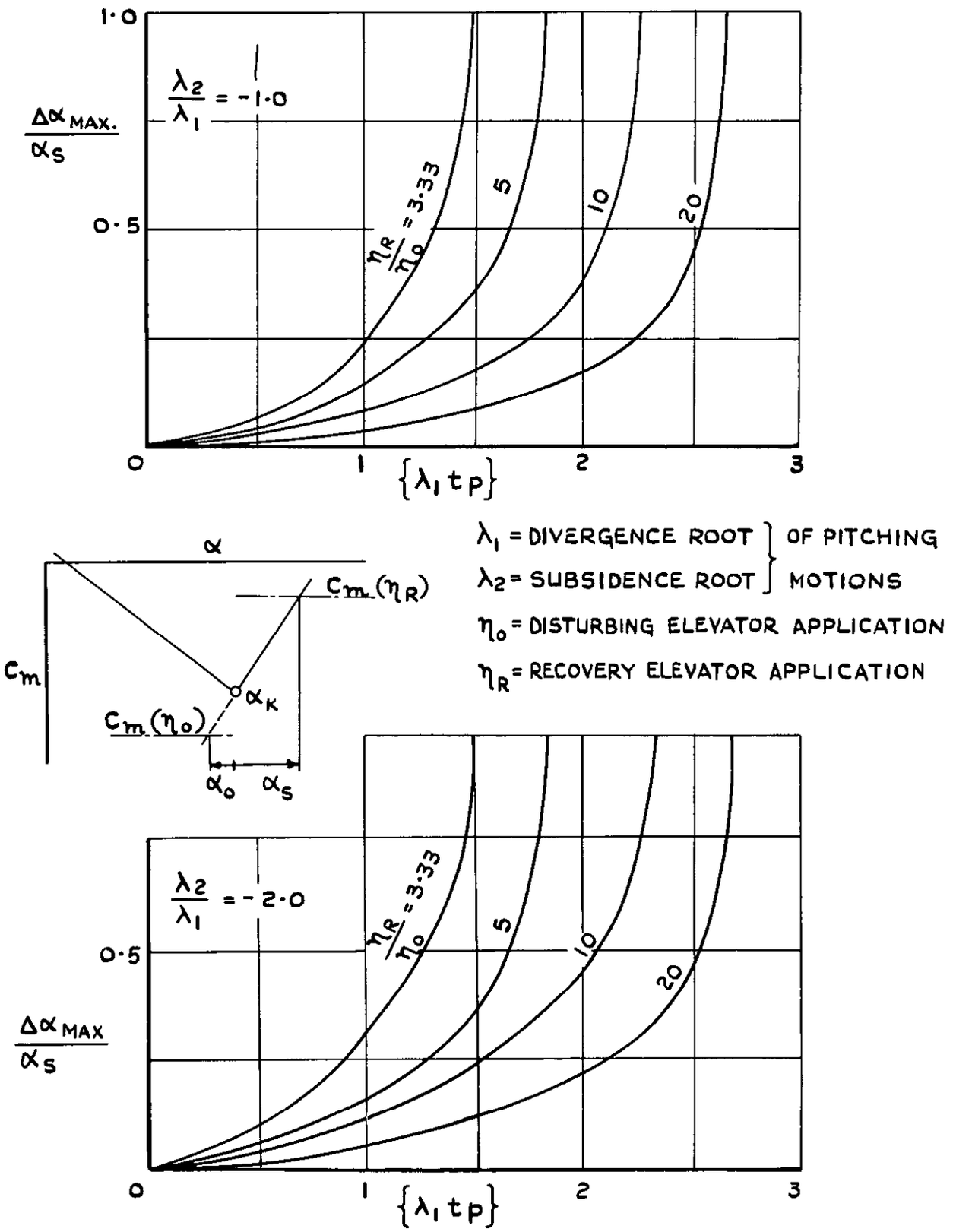

FIG. 29. PEAK OVERSHOOT AMPLITUDE IN PITCH UP WHERE PILOT'S RECOVERY ACTION FOLLOWS WITH A TIME DELAY OF t_p SECONDS.

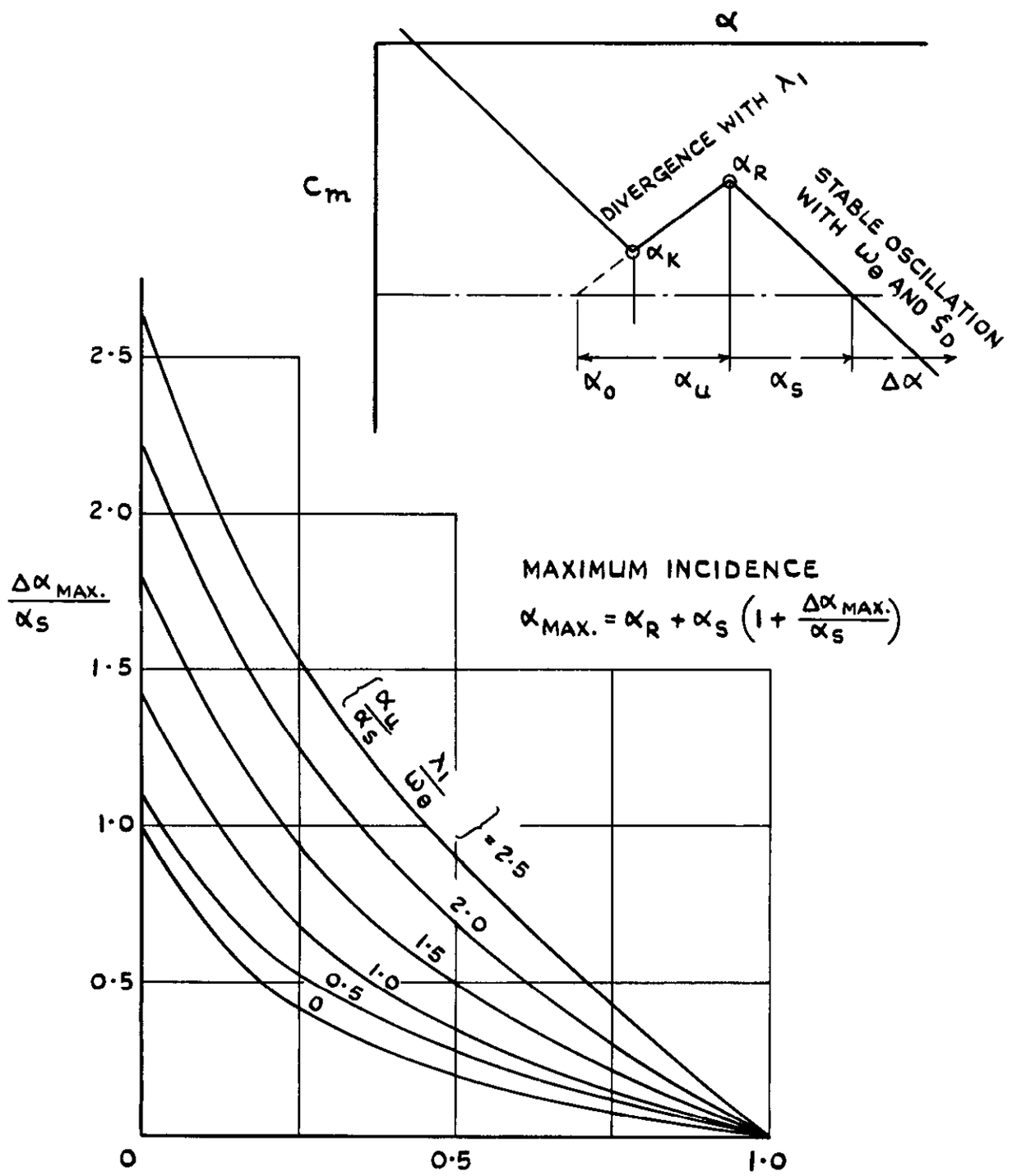

FIG.30. OVERSHOOT AMPLITUDE $\Delta\alpha$ IN PITCH UP WITHOUT PILOTS CORRECTIVE ACTION.

C.P. No. 404
(19,942)
A.R.C. Technical Report

Published by
HER MAJESTY'S STATIONERY OFFICE

To be purchased from
York House, Kingsway, London w.c 2
423 Oxford Street, London w.1
13A Castle Street, Edinburgh 2
109 St Mary Street, Cardiff
39 King Street, Manchester 2
Tower Lane, Bristol 1
2 Edmund Street, Birmingham 3
80 Chichester Street, Belfast
or through any bookseller

PRINTED IN GREAT BRITAIN

S.O. Code No. 23-9011-4

C.P. No. 404